Smooth and Nonsmooth Bifurcations in Welander's Ocean Convection Model

A THESIS
SUBMITTED TO THE FACULTY OF THE GRADUATE SCHOOL
OF THE UNIVERSITY OF MINNESOTA
BY

Juliann Kay Leifeld

IN PARTIAL FULFILLMENT OF THE REQUIREMENTS
FOR THE DEGREE OF
Doctor of Philosophy

May, 2016

© Juliann Kay Leifeld 2016
ALL RIGHTS RESERVED

Acknowledgements

First and foremost, I must thank Richard McGehee, without whom this would not have been possible. In addition to being my most important mathematical consultant, he has been a mentor and friend to me throughout this journey, and his support has been the most important factor in my success.

The support I have received from my family also can't be overstated. They believed in me even when I didn't believe in myself, and their encouragement helped me carry on through good times and bad.

Finally, I must thank my friends and compatriots: Kaitlin Hill and Andrew Roberts for making mathematical collaboration something to look forward to, Samantha Oestreicher, Bryan Poling, and Alanna Hoyer-Leitzel for making dynamical systems fun to learn, Gabriela Jaramillo for her quiet commiseration and for being the best office mate, Nicole Bridgland for taking me hiking when I needed to forget about work for a while, and Caitlin Weixel, Amy Gehring, Christine Boone, and Allison Drtina for keeping me sane by reminding me that there's more to life than mathematics.

Abstract

Welander's model is a conceptual ocean convection model, that describes ocean convection with a few, simple dynamical equations. Welander's goal in formulating his model was to show that internally driven oscillations could be caused solely by switching between strongly convective and nonconvective states. Because of the conceptual importance of the switching mechanism, Welander created two versions of the model, one with a smooth transition between convective states, and one with an abrupt nonsmooth transition. He was able to numerically find a periodic orbit in both versions of the model. The climactic import of the model is in the idea that oscillations can be internally driven, but the model also has interesting mathematical import. Welander's implicit assumption that the nonsmooth model is easier to analyze is mathematically suspect, and a rigorous comparison between the smooth and nonsmooth models is not immediately clear. In this work, we introduce the model with scientific context, and complete a rigorous nonsmooth analysis of the model. We find one known nonsmooth bifurcation analogous to a supercritical Hopf bifurcation, but we also find a bifurcation that has not been previously described. Finally, we compare the smooth and nonsmooth models, paying close attention to the dangers inherent in such a comparison.

Contents

List of Figures

Chapter 1

Introduction

- Chapter 2 introduces the convection model, with some scientific context and initial analysis.
- Chapter 3 outlines methods of analysis of nonsmooth dynamical systems.
- In Chapter 4 the bifurcation structure of Welander's nonsmooth model is analyzed.
- Chapter 5 discusses the difficulties inherent in comparing smooth and nonsmooth dynamical systems.
- Chapter 6 relates the smooth and nonsmooth versions of the first bifurcation in Welander's model.
- Chapter 7 compares the smooth and nonsmooth versions of the second bifurcation in Welander's model.
- Chapter 8 discusses the results presented in the thesis, and proposes future work. thesis.

Chapter 2

Welander's Model

2.1 Ocean Circulation Box Models

Ocean circulation is a fundamental component of the Earth climate system. It plays a key role in distributing heat and moisture around the globe, and even small changes in circulation patterns can have a huge effect on both global and regional climates. This has been seen in a number of modern events, most notably El Nino phenomena. Additionally, some paleo phenomena, such as Dansgaard Oeschger (DO) events, can be tied to changes in ocean dynamics and cause global changes in temperature [1, 2, 3]. In many cases, these changes in ocean circulation are seen as oscillations in the climate record, on a variety of time scales. For example, DO events are a periodic strengthening and weakening of the Atlantic Meridional Overturning Circulation (AMOC) or gulf stream, which are seen in the climate record during the last glacial maximum. They have a period of around 1500 years, and are inferred through proxy temperature data from the European continent. The oscillations are thought to be caused by a sudden influx of fresh water into the atlantic, and can be well modeled as a relaxation oscillation in a low dimensional model of temperature and salinity in the AMOC. Alternatively, there is periodic variability of smaller magnitude in the strength of the gulf stream, occuring on a shorter time scale of 60 years[4, 5, 6]. Because the gulf stream is a major transporter of heat from the equator to the European continent, changes in the strength of this circulation pattern have direct impacts on European and northern hemispheric climate patterns. These effects may also have more complicated consequences for systems relying

on regular climate patterns, such as agriculture.

Because ocean circulation plays such an important role in global climate dynamics, it is important to be able to model and explain the internal variabilities in the ocean system. Climate models are split into general categories based on their level of complexity, each having both benefits and drawbacks. At one end of the scale, conceptual climate models have a relatively small number of low dimensional equations. These models don't capture details in the global climate system, but can quite accurately describe large scale phenomena. Alternatively, global climate models or GCMs can have many thousands of equations, and can model detail on relatively small spatial scales. However, it is difficult to fully understand the model when it is that complicated, so there is little confidence that all aspects of the system are accurate. However, even with their drawbacks both types of models can give important scientific information. The book by Kaper and Engler gives a good introduction to mathematical approaches in climate modeling [7].

In the realm of conceptual ocean circulation models, Welander's model has had import in the climate community for demonstrating internally driven oscillatory behavior in a simple system [8]. Welander's model is an ocean circulation box model, meaning it splits the ocean into regions, or boxes. The water in each box is assumed to be well mixed, and ordinary differential equations describe the flow of water from one box to the other, usually due to pressure caused by density differences between the boxes. In an ocean circulation box model, the only relevant variables are temperature and salinity of the water in each box, and density is described as an equation of state, usually a linear combination of the variables. These models have been used to describe both large and small scale changes in the AMOC, like DO events and the previously mentioned 60 year oscillation. Welander's model describes convection between the surface ocean and the deep ocean, and showed that oscillation in convection strength could be the sole result of a switching threshold between convective and nonconvective modes. Then, strong or weak convection could drive larger circulation patterns, changing global circulation strength.

In addition to developing a smooth model, Welander formulated a nonsmooth version of his model, to represent abrupt switching between convective states. This type of approximation seems scientifically natural, and is seen in many different applications

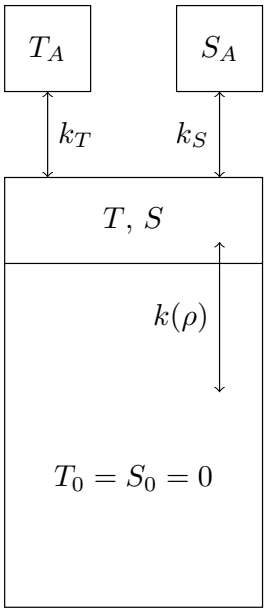

Figure 2.1: A schematic of Welander's Model. The temperature and salinity of the surface ocean are forced by atmospheric temperature (T_A) and by salinity forcing in the form of precipitation and evaporation (S_A). The surface box mixes convectively with the deep ocean via the convection function $k(\rho)$.

in climate science [9, 10, 11, 12]. However, the approximation raises some interesting mathematical questions. In the following sections, we describe and analyze Welander's model from a mathematical perspective.

2.2 Description of Welander's Model

Welander's model is a standard ocean circulation box model (see Figure 2.1) [8]. The model separates the ocean into two regions, a surface ocean and a deep ocean. The relative density of the water in the boxes dictates the interaction between them, and the density is controlled by the temperature and salinity of the water, through an equation of state: $\rho = -\alpha T + \beta S$. The deep ocean is assumed to have constant density ($T_0 = S_0 = \rho_0 = 0$). The surface ocean box is assumed to be well mixed, and so the circulation dictated by the equations must represent large scale behavior, where the vagaries of the density don't play a major role. Equations for the temperature and

salinity in each box can then be written as

$$\begin{aligned} \frac{dT}{dt} &= k_T(T_A - T) - k(\rho)T \\ \frac{dS}{dt} &= k_S(S_A - S) - k(\rho)S \\ \rho &= -\alpha T + \gamma S. \end{aligned} \tag{2.1}$$

T_A and S_A are generic atmospheric forcing caused by precipitation, evaporation, solar forcing, etc, and are assumed to be constant. The key feature of Welander's model is the convective mixing function $k(\rho) \geq 0$, which could be smooth, or piecewise smooth. Welander assumes that convection is small when the density of the surface ocean is small, large when the density is large, and the transition between these states is abrupt. These are reasonable assumptions, because the ocean is in general highly stratified, without much mixing between the layers. It is this switching behavior that allows for periodicity in Welander's model.

Although the model doesn't have many parameters, it is still useful to nondimensionalize it. We make the following coordinate change

$$T^* = \frac{T}{T_A}, \quad S^* = \frac{S}{S_A}, \quad \rho^* = \frac{\rho}{\gamma S_A}, \quad t^* = k_T t,$$

which results in the system

$$\begin{aligned} \dot{T} &= 1 - T - \frac{k(\rho)}{k_T}T \\ \dot{S} &= \frac{k_S}{k_T}(1 - S) - \frac{k(\rho)}{k_T}S \\ \rho &= \frac{-\alpha T_A}{\gamma S_A}T + S. \end{aligned}$$

Renaming the parameters, we obtain the nondimensionalized form of Welander's model,

$$\begin{aligned} \dot{T} &= 1 - T - k(\rho)T \\ \dot{S} &= \beta(1 - S) - k(\rho)S \\ \rho &= -\alpha T + S. \end{aligned} \tag{2.2}$$

2.3 General Analysis of the Model

Welander does some basic analysis on the model given by (2.1), to show the existence of a periodic orbit when k is smooth. Given some conditions on the function k and on the parameters, one can prove that a unique unstable equilibrium exists.

The equilibria occur when

$$\overline{T} = \frac{T_A k_T}{k_T + \overline{k}}$$
$$\overline{S} = \frac{k_S S_A}{k_S + \overline{k}},$$

where $\overline{k} = k(\overline{\rho})$. Plugging these into the equation of state from (2.1), we get an equation for the equilibria depending only on ρ.

$$\overline{\rho} = -\alpha\overline{T} + \gamma\overline{S} = -\frac{\alpha T_A k_T}{k_T + \overline{k}} + \frac{k_S \gamma S_A}{k_S + \overline{k}} = F(\overline{\rho}) \tag{2.3}$$

Depending on the shape of k, there can be one or many equilibria. In analyzing this model, the goal is to find a periodic solution. If the model only has one equilibrium, and it is unstable, the Poincare-Bendixson theorem gives the existence of a stable periodic orbit.

It can be shown that any rectangle $(-T_0, T_0) \times (-S_0, S_0)$ with $T_0 > T_A$ and $S_0 > S_A$ is forward invariant. We show this as follows: $k(\rho) \geq 0$ for all ρ, so k must have an infimum k^* on our rectangle. In the region where $T > 0$, the right hand side of the $\dot{T}$ equation along the rectangle boundary is then

$$k_T T_A - k_T T_0 - k(\rho) T_0 \leq k_T T_A - (k_T + k^*) T_0 < 0$$

because $T_0 > T_A$ and $k > 0$. A similar inequality can be formulated in S_0. Likewise when $T < 0$,

$$k_T T_A - k_T T_0 - k(\rho) T_0 = k_T |T_0| + k_T T_A + k(\rho)|T_0| \geq k_T |T_0| + k_T T_A + k^* |T_0| > 0$$

Therefore, the vector field on the boundary of the rectangle points inward, and we have an invariant set.

We use (2.3) to look for cases with a single unstable equilibria. A sufficient but unnecessary condition is $F'(\overline{\rho}) < 1$, or

$$\left[\frac{\alpha T_A k_T}{(k_T + \overline{k})^2} - \frac{k_S \gamma S_A}{(k_S + \overline{k})^2}\right] \overline{k}' < 1$$

Here, $\overline{k}' = k'(\overline{\rho})$.

Assuming k is differentiable, the linearized system is

$$\begin{bmatrix} w' \\ z' \end{bmatrix} = \begin{bmatrix} -(k_T + k(\overline{\rho})) + \overline{T}\alpha k'(\overline{\rho}) & -\overline{T}\gamma k'(\overline{\rho}) \\ \overline{S}\alpha k'(\overline{\rho}) & -(k_S + k(\overline{\rho})) - \overline{S}\gamma k'(\overline{\rho}) \end{bmatrix} \begin{bmatrix} w \\ z \end{bmatrix}$$

To get instability of our equilibrium, we must find parameters such that the trace of the matrix is positive. This condition gives

$$-k_T - k + \overline{T}k'\alpha - k_S - k - \overline{S}k'\gamma > 0,$$

or, after some simplification,

$$k_S + k_T + 2k + \overline{\rho}k' < 0.$$

For this to be true we must have $\overline{\rho} < 0$, i.e. the equilibrium is in a weak convection state. Parameters can be found where this condition is satisfied.

2.4 Welander's Analysis for a Specific Smooth Function k

To continue his analysis, Welander uses (2.2), and chooses two specific functions for $k(\rho)$, one continuous, and one discontinuous. The smooth k is

$$k(\rho) = \frac{1}{\pi}\tan^{-1}\left(\frac{\rho - \varepsilon}{a}\right) + \frac{1}{2} \tag{2.4}$$

and the nonsmooth k is

$$k(\rho) = \begin{cases} k_1 & \rho > \varepsilon \\ 0 & \rho < \varepsilon \end{cases} \tag{2.5}$$

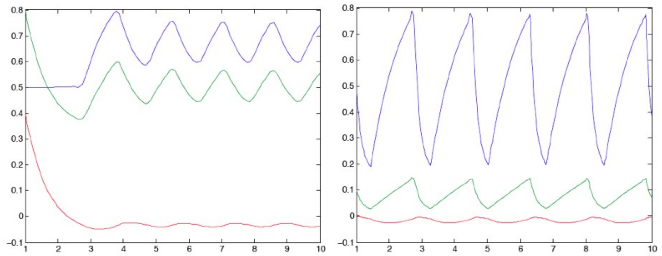

(a) (b)

Figure 2.2: The periodic orbit found numerically in the (A) smooth case, and the (B) nonsmooth case. The top blue curve is the temperature, the middle green curve is salinity, and the lower red curve is density.

Both of these satisfy the qualitative assumption made earlier, in which k should be large only past a certain surface ocean density threshold. k is defined to be a monotonically increasing, positive function, which acts like a switch between states of convection and nonconvection. Analyzing the smooth model using the parameters

$$\beta = \frac{1}{2} \quad \alpha = \frac{4}{5} \quad a = \frac{1}{500} \quad \varepsilon = -\frac{1}{30},$$

it can be easily verified that the equilibrium occurs at

$$T = 2/3 \quad S = 1/2 \quad \rho = -1/30.$$

Calculating the eigenvalues for the linearlized system we find that this is an unstable equilibrium, so the system contains a stable periodic orbit. Welander finds this orbit numerically, as shown in Figure 2.2A.

2.5 Welander's Analysis for a Specific Nonsmooth k

Although the previous analysis does not apply because of the discontinuity, Welander still numerically finds a periodic orbit when k is nonsmooth, using (2.5). The mathematical mechanism behind this oscillation is different in the nonsmooth, or *flip flop* model, which has a phase portrait as seen in Figure 2.3. Because k has two different

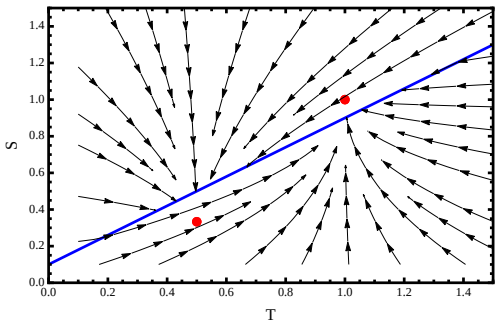

Figure 2.3: The phase portrait of Welander's model, using the parameters given in (2.6), with $\varepsilon = -0.1$. The blue line indicates the nonsmooth boundary between convective states. The red dots are the equilibria for each region, whose existence in the opposite region of space seems to drive the oscillation in the model.

constant values, dependent on the region, the dynamical system becomes completely decoupled, except that the boundary at which the system switches is dependent on both T and S. This makes it incredibly easy to find two different equilibria for each region of space. The oscillations are then caused by the fact that for certain parameter values these stable equilibria don't exist in the region of phase space for which they are equilibria. Therefore, as the system approaches the equilibrium, it crosses the discontinuity line, and then reverses direction to approach the other equilibrium. This can lead to a stable routine of switching between states. Welander does not discuss the mathematics behind the flip flop model with rigor, but numerically finds a periodic solution, using the parameters

$$\beta = \frac{1}{10} \quad \alpha = \frac{1}{5} \quad k_1 = 5 \quad \varepsilon = -\frac{1}{100}.$$

The numerical solution can be seen in Figure 2.2B.

It is clear that Welander chooses to analyze a nonsmooth version of his model because he believes it to be easier than the analysis of the smooth model. From some perspectives this is obvious, as the nonsmooth model has decoupled equations, and the systems on each side of the discontinuity are quite simple. However, Welander does not discuss the mathematical implications of the use of a nonsmooth system, and does not do a full analysis of this system. In fact, it is not mathematically obvious that the smooth and the nonsmooth system display the same qualitative behavior in all parameter ranges. It is also troubling that Welander uses different parameter values to display the same type

of oscillation, which indicates that there may be some trouble in comparing the smooth and nonsmooth systems. In the following chapters, we will complete a rigorous analysis of the bifurcation structure of the nonsmooth system, and compare this structure to the smooth system. We will unify the parameter choices between the systems, choosing the parameters that Welander uses to analyze the smooth model,

$$\alpha = \frac{4}{5} \quad \beta = \frac{1}{2} \quad k_1 = 1. \tag{2.6}$$

This also ensures that the nonsmooth system is the pointwise limit of the smooth system as $a \to 0$, and the systems can be compared. ε will be the bifurcation parameter. Choosing α and β as given limits the scope of the bifurcation analysis for these results. Future work should include a study of the possible bifurcation structures when these values vary.

Chapter 3

Nonsmooth Analysis Fundamentals

3.1 Solutions to Nonsmooth Systems

To complete an analysis of the nonsmooth system, we must first discuss the methods used in such an analysis. Because all of the results pertain to two dimensional nonsmooth systems, we will discuss the background in this context. In general, a piecewise smooth system can be written in the form

$$\dot{x} = f(x, \lambda) \tag{3.1}$$

with f a vector function depending on the variable x and a nonsmooth function λ,

$$\lambda = \begin{cases} 1 & h(x) > 0 \\ 0 & h(x) < 0. \end{cases} \tag{3.2}$$

$h(x)$ is a scalar function which defines the location of the discontinuity curve, or *splitting manifold*. We define the vector fields on either side of the discontinuity as $f_1(x) = f(x, 1)$, and $f_0(x) = f(x, 0)$.

Behavior of the system away from the splitting manifold can be determined using classical methods, but along the splitting manifold new dynamics must be defined. Here we use Filippov's convex combination method [13]. If the vector fields on either side

of the splitting manifold point in the same direction, one expects trajectories there to cross, and we call this a *crossing region*. Alternatively, if both vector fields point either toward or away from the splitting manifold, trajectories slide along the manifold, and we call this a *sliding region*. Sliding regions exist when the system of equations

$$\begin{aligned} S = f(x;\lambda)\cdot\nabla h(x) = 0 \\ h(x) = 0. \end{aligned} \tag{3.3}$$

can be solved for $\lambda \in [0,1]$. When $f(x,\lambda)$ has a linear dependence on λ, as in the convex combination

$$f(x,\lambda) = \lambda f_1(x) + (1-\lambda) f_0(x),$$

equation (3.3) corresponds to locations for which the convex combination of the vector fields contains a vector in the direction of the splitting manifold. The boundaries of the sliding region are located in places where the vector fields given by $f_0(x)$ and $f_1(x)$ are tangent to the splitting manifold, i.e. where the vector fields change direction relative to the manifold. Stability of the sliding region itself can be found using (3.3). If

$$\frac{d}{d\lambda} S < 0$$

then the sliding region is stable, and if

$$\frac{d}{d\lambda} S > 0$$

the sliding region is unstable. Figure 3.1 shows a schematic example of an unstable sliding region.

Sliding flow along the splitting manifold can be determined by solving (3.3) for $\lambda^*(x)$, then looking at the dynamics of

$$\dot{x} = f(x, \lambda^*(x)). \tag{3.4}$$

Dynamical phenomena in the sliding region can then be determined from (3.4) in the normal way. Equilibria of equation (3.4) are called *pseudoequilibria*. These pseudoequilibria are *pseudonodes* if they are nodes in the Filippov flow and their Filippov stability

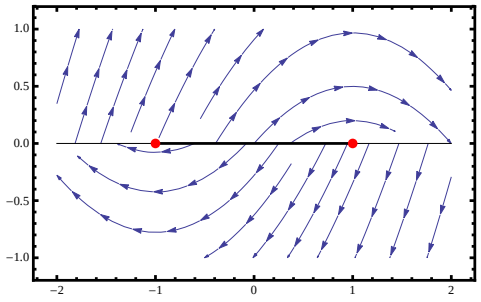

Figure 3.1: Schematic of an unstable sliding region. Boundaries of the sliding region (red dots) occur when one of the vector fields is tangent to the splitting manifold. Stability is determined by the direction of the vector fields on either side of the sliding region.

agrees with the stability of the sliding region. Otherwise they are called *pseudosaddles*. Although eigenvalues and eigenvectors for pseudoequilibria are nonstandard, convergence rates can be determined within the sliding region in the normal way, by analyzing (3.4). In the direction normal to the sliding region, convergence or divergence generally happens in finite time, unless the pseudoequilibrium is coincident with an equilibrium of $f_0(x)$ or $f_1(x)$. This coincidence is called a *border collision*, and will be discussed further in the next section.

Solutions to the full system (3.1) are in general not unique. If the sliding region is stable, many different solutions will converge there in finite time, and then overlap according to the defined vector field on the splitting manifold. If the sliding region is unstable, an initial condition on the splitting manifold can lead to a whole family of solutions, which slide an arbitrary distance in the sliding region, before escaping into either region of phase space.

3.2 Bifurcations in Nonsmooth Systems

In addition to the standard bifurcations which can occur in smooth regions of phase space, or in the dynamics of the sliding flow, there are many novel types of bifurcations in nonsmooth systems. Some work has been done to classify codimension one bifurcations of piecewise smooth systems, but this work is far from complete. Here we will discuss what is known so far.

3.2.1 Classifying Nonsmooth Bifurcations and Normal Forms

The mathematical basis for analyzing nonsmooth systems is relatively young, and so rigorous classification of nonsmooth bifurcations is not yet done. There are many potential obstacles to using normal forms in nonsmooth systems. The most critical is a lack of systematic inspection of relevant equivalencies. Many sources use topological equivalence as a standard, but that severely limits the scope of bifurcation analysis. If a system is piecewise smooth, it might be reasonable to use piecewise smooth transformations, however these transformations are likely to destroy sliding behavior, which is necessary to many types of nonsmooth bifurcation. Continuous transformations can preserve sliding behavior, however, the angles of the vector fields relative to the splitting manifold have been shown to be crucial in several cases, including the border collision described in Section 4.3. This lack of rigorous mathematical background poses serious problems to the classification of bifurcations, and as a result, the field now consists mostly of examples of possible phenomena. There has been some assumption of normal forms, as in [14, 15], however these classifications miss some crucial cases, and a rigorous discussion of the mathematics behind the "normal forms" is not included. The work of Jeffrey [16, 17] has also exposed some issues with normal forms, related to a phenomenon called *nonlinear sliding*. He proved that every nonsmooth system is the pointwise limit of infinitely many smooth systems, each with identical behavior away from the splitting manifold. This will be discussed in more detail in Section 5.1. Jeffrey's result indicates that knowledge of the vector fields in the smooth regions of phase space is not sufficient to determining behavior on the splitting manifold. In particular, if one uses the Filippov formulation described in Section 3.1, nonlinear transformations will not preserve this formulation, and qualitatively different behavior might be introduced. This also indicates that care must be taken in attempting to define normal forms. Therefore, the work here is descriptive instead of prescriptive. The next section will describe some relevant known nonsmooth bifurcations.

3.2.2 Some Relevant Nonsmooth Bifurcations

One of the basic types of nonsmooth bifurcation is the *double tangency*, shown in Figure 3.2. This is a self descriptive way to say that tangencies of f_1 and f_0 occur simultaneously

in space. The behavior as the parameter is perturbed away from the bifurcation is dependent on whether the tangencies are *visible* or *invisible*. A visible tangency is one where the trajectory through the tangent point exists in the region of phase space containing the vector field with the tangency. An invisible tangency is one where this trajectory exists in the opposite region of phase space. So, a double tangency can involve two visible tangencies, two invisible, or one of each. In all of these cases, interesting behavior is also dependent on the directions of the vector fields at the tangencies. If at least one of the tangencies is visible, the bifurcation will in general affect location and/or existence of pseudoequilibria and the sliding region. These cases are discussed in several sources, but are not immediately relevant to our results, so will not be discussed in detail here [18, 15, 19, 14, 20, 13, 21]. Of more immediate interest is the double invisible tangency, or *fused focus* bifurcation, which is also discussed in the above sources. In this bifurcation, two invisible tangencies cross, causing a sliding region to narrow to a point and change stability as the parameter moves through the bifurcation. The sliding region will generally also contain a pseudonode which persists, but changes stability. The change in stability then creates a small periodic orbit, which grows as the parameter changes, analogous to a standard, smooth Hopf bifurcation. This bifurcation has been known at least since 1980 [13], however a normal form for the bifurcation has not been rigorously proven, due to the constraints previously mentioned.

Another relevant nonsmooth bifurcation is called a *border collision* bifurcation. In this bifurcation, a real equilibrium collides with a splitting manifold. The outcome of such a bifurcation depends on the stability of the real equilibrium, and so it is generally split into cases; border node, border saddle, and border focus. In much of the literature, attention is given to *persistence* of the equilibrium, usually as a pseudoequilibrium. In fact, it has been stated in [15, 14] that there are only two possible relevant outcomes in the border node, annihilation and persistence. In the case where the equilibrium persists as a pseudoequilibrium, the stability of the equilibrium remains unchanged, in that an attractor remains an attractor, and a repeller a repeller. However, we will see in Section 4.3 that other possibilities exist. This is just one more caution that bifurcation classification in nonsmooth systems is far from complete.

In the following chapter, we will use this formulation of nonsmooth systems to analyze the bifurcation structure of Welander's Model.

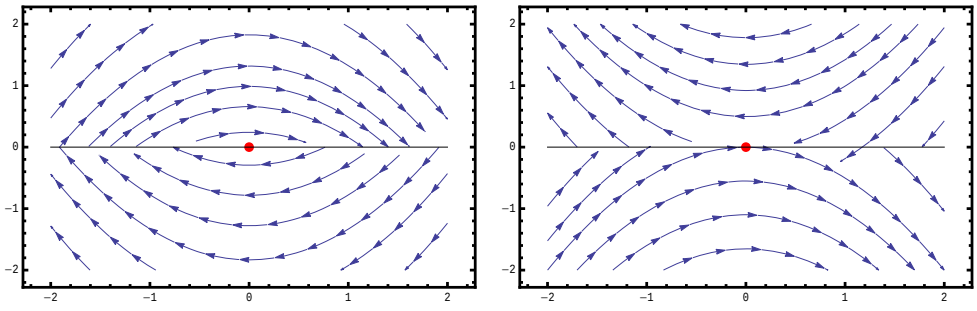

(a)

(b)

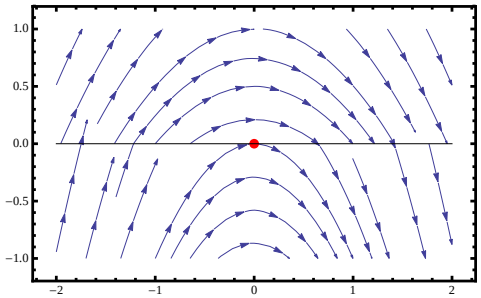

(c)

Figure 3.2: Schematic examples of double tangencies. The tangencies can be both invisible, both visible, or a mix of visible and invisible.

Chapter 4

A Rigorous Treatment of Welander's Nonsmooth Model

4.1 A Preliminary Coordinate Change

We start with the nondimensionalized nonsmooth version of Welander's model (2.2),

$$\begin{aligned} \dot{T} &= 1 - T - k(\rho)T \\ \dot{S} &= \beta(1 - S) - k(\rho)S, \end{aligned}$$

$$k(\rho) = \begin{cases} 1 & \rho > \varepsilon \\ 0 & \rho < \varepsilon, \end{cases}$$

$$\rho = -\alpha T + S.$$

This is in the standard form seen in (3.2), where $\lambda = k$. Because the splitting manifold, which is the line $\rho = -\alpha T + S = \varepsilon$, depends explicitly on the bifurcation parameter ε, it is useful to the analysis to do an initial change of coordinates, with $y = \rho - \varepsilon$, or

$$\begin{aligned} x &= T \\ y &= S - \alpha T - \varepsilon, \end{aligned}$$

after which the splitting manifold is the line $y = 0$. With the following basic calculation

$$\begin{aligned}\dot{y} = \quad \dot{S} - \alpha\dot{T} &= \beta(1-S) - kS - \alpha(1-T-kT) \\ &= \beta(1-S) - k(S-\alpha T) - \alpha + \alpha T \\ &= \beta(1-S) - k(y+\varepsilon) - \alpha + \alpha T \\ &= \beta(1-y-\alpha T-\varepsilon) - k(y+\varepsilon) - \alpha + \alpha T \\ &= \beta - \beta\varepsilon - k\varepsilon - \alpha - (\beta+k)y - (\alpha\beta-\alpha)T.\end{aligned}$$

Because $\rho = -\alpha T + S$, the function $k(\rho)$ under the coordinate change becomes

$$k(y) = \begin{cases} 1 & y > 0 \\ 0 & y < 0. \end{cases}$$

The splitting manifold is given by the scalar function $h(x, y) = y = 0$. Then, letting $T = x$, the system is

$$\begin{aligned}\dot{x} &= 1 - x - k(y)x \\ \dot{y} &= \beta - \beta\varepsilon - k\varepsilon - \alpha - (\beta+k)y - (\alpha\beta-\alpha)x \\ k(y) &= \begin{cases} 1 & y > 0 \\ 0 & y < 0 \end{cases}.\end{aligned} \tag{4.1}$$

It is important to note that this coordinate change is a linear transformation composed with a translation. Neither the translation or the linear transformation change the Filippov analysis of the nonsmooth system. That the translation doesn't change the Filippov analysis is obvious. We see that the linear transformation maps the original Filippov vector field into the new Filippov vector field as follows. Fixing x, the original system has three relevant vectors at the point x, the vector given by the $k = 1$ vector field, the vector given by $k = 0$, and the Filippov vector v. It is only necessary to show that the transformation of the Filippov vector, $\overline{v}$, remains parallel to the $h(x) = 0$ manifold under the transformation, and that $\overline{v}$ remains in the convex combination of the transformation of f_1 and f_2. The fact that $\overline{v}$ remains parallel to the $h(x) = 0$ manifold is obvious. Showing that the new vector remains in the convex combination is

also straightforward, because

$$\overline{v} = DLv = DL\left(\lambda f_1 + (1-\lambda) f_2\right) = \lambda DLf_1 + (1-\lambda) DLf_2.$$

4.2 The Fused Focus

Theorem 1. *When $\varepsilon = 0$, the nonsmooth system* (4.1) *with k given by* (2.5) *and parameters* (2.6) *contains a fused focus bifurcation.*

Proof. The boundaries of the sliding region are given by points where $\dot{y} = 0$ along $y = 0$, which gives the equation

$$0 = \beta + \beta\varepsilon - k\varepsilon - \alpha - (\alpha\beta - \alpha)x.$$

Solving this equation for x, and plugging in the values for α and β given in (2.6), and $k = 0$ or $k = 1$, we find that the sliding region has boundaries

$$x = \frac{3}{4} + \frac{15}{4}\varepsilon,$$

and

$$x = \frac{3}{4} + \frac{5}{4}\varepsilon.$$

This shows that the sliding region collapses to a single point in the case $\varepsilon = 0$.

Stability of the sliding region is given by (3.3). In the context of Welander's model, $\lambda = k$, and because of the coordinate change, we can choose $h = y$, which will satisfy all of the stipulations laid out in Chapter 3. Here,

$$\frac{d}{d\lambda}(f \cdot \nabla h)|_{y=0} = \frac{d}{dk}\left(\beta - \beta\varepsilon - k\varepsilon - \alpha - (\beta + k)y - (\alpha\beta - \alpha)x\right)|_{y=0} = -\varepsilon.$$

This indicates that the sliding region is stable for $\varepsilon > 0$ and unstable for $\varepsilon < 0$ (see Figure 4.1). It is reasonable that this change in stability occurs simultaneously to the sliding region narrowing to a point before expanding again.

The fused focus bifurcation is dependent on both tangencies being *invisible* when $\varepsilon = 0$, meaning that the trajectory through the tangency does not exist in that region of phase space. This allows for the double tangency to be a focus, as opposed to a saddle

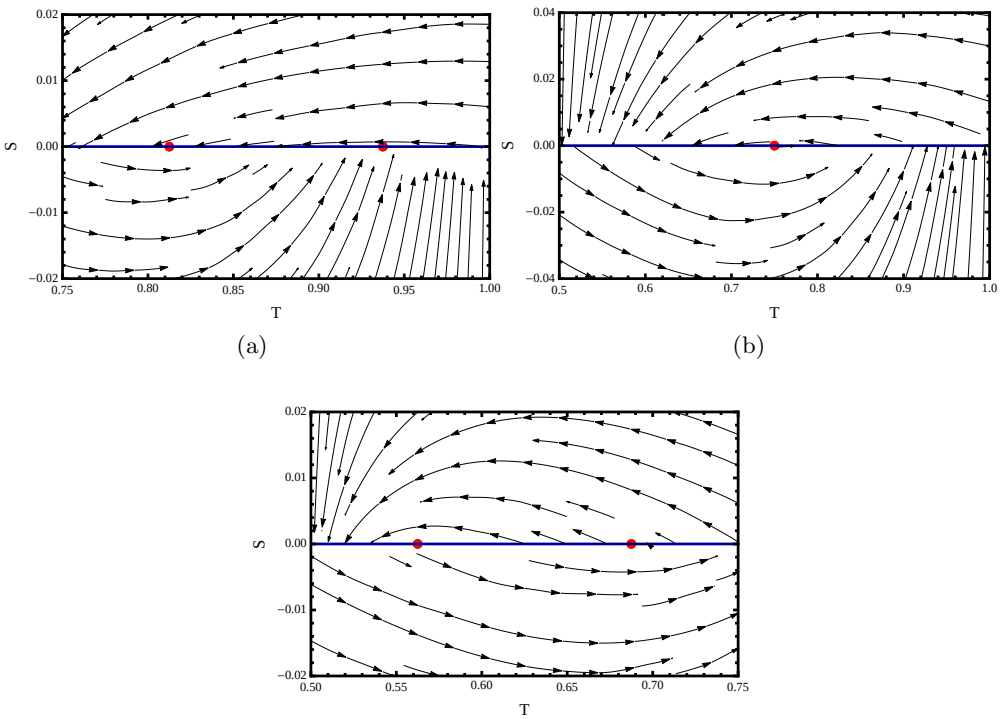

Figure 4.1: The stability of the sliding region in system (4.1). In (A) $\varepsilon = 0.05$ and the sliding region is stable. In (B) there is a double tangency when $\varepsilon = 0$, and in (C) $\varepsilon = -0.05$, and the sliding region is unstable.

or some mixture of the two. It is easy to see that the double tangency is invisible. The x derivative of the phase curves along $y = 0$ is

$$\frac{dy}{dx} = \frac{\beta - \beta\varepsilon - k\varepsilon - \alpha - (\alpha\beta - \alpha)x}{1 - x - kx}.$$

In the region where $k = 1$, when

$$x > \frac{3}{4},$$

$$\frac{dy}{dx} < 0,$$

and when

$$\frac{1}{2} < x < \frac{3}{4},$$

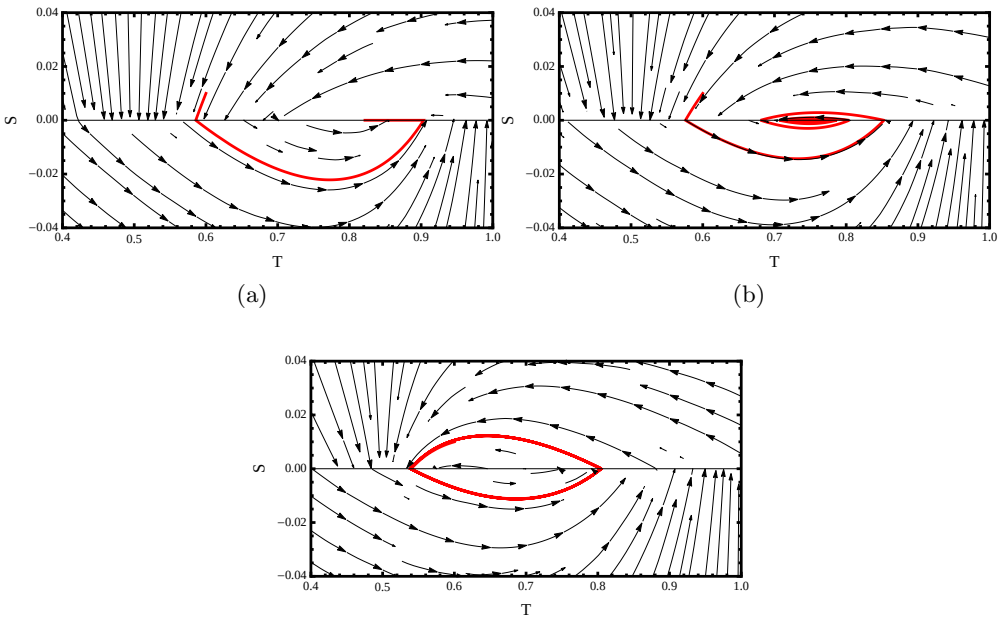

(a) (b)

(c)

Figure 4.2: The birth of a periodic orbit through the fused focus bifurcation. (A) When $\varepsilon = 0.04$, trajectories converge to the stable sliding region. (B) When $\varepsilon = 0$, trajectories converge to a stable focus. (C) When $\varepsilon = -0.04$, trajectories converge to a stable periodic orbit.

$$\frac{dy}{dx} > 0,$$

so the function has a local maximum at the tangency. For $k = 0$ and

$$x < \frac{3}{4},$$

$$\frac{dy}{dx} < 0,$$

and for

$$\frac{3}{4} < x < 1,$$

$$\frac{dy}{dx} > 0,$$

implying the function has a local minimum.

Filippov gave conditions on the stability of the fused focus [13]. Expanding each vector field around the fused focus, we write

$$\frac{dy}{dx} = ax + by + cx^2 + dxy + ey^2 + \phi(x, y)$$

where each coefficient has two values, depending on the region of phase space. Then, we let

$$A_{1,0} = \frac{2}{3}\left(b_{1,0} - \frac{c_{1,0}}{a_{1,0}}\right)$$

with the subscript indicating the k value. A sufficient, but not necessary condition for stability of the fused focus is $A_1 - A_0 < 0$. In Welander's model, evaluated at $\varepsilon = 0$,

$$\begin{aligned}\frac{dy}{dx} = \quad & \frac{8}{5\,(3k-1)}\left(x - \frac{3}{4}\right) + \frac{2(1+2k)}{3k-1}y + \frac{32(1+k)}{5(3k-1)^2}\left(x - \frac{3}{4}\right)^2 \\ & -\frac{8\left(1+3k+2k^2\right)}{(3k-1)^2}\left(x - \frac{3}{4}\right)y + \phi(x, y).\end{aligned}$$

So,

$$A = \frac{2}{3}\left(b - \frac{c}{a}\right) = \frac{-4}{9k-3}$$

which gives

$$A_1 - A_0 = -2 < 0,$$

so the fused focus is stable. Then, the changing stability of the sliding region as ε becomes negative immediately gives the existence of a small periodic orbit nearby. □

In Theorem 1 we conclude the existence of a periodic orbit as the system undergoes the bifurcation. A constraint on the location of the periodic orbit will be proven in Theorem 4. The uniqueness of the periodic orbit is not immediately clear, although simulations indicate that it is likely to be unique. Figure 4.2 shows trajectories of the system as it undergoes the fused focus bifurcation. So, we see a nonsmooth version of a supercritical Hopf bifurcation using a Filippov analysis of Welander's model.

4.3 Border Collision

4.3.1 Local structure

Oscillation in Welander's model is predicated on attraction to two different virtual equilibria. However, it is immediately clear that parameter changes can transition these virtual equilibria into globally stable, real equilibria. The location of the virtual equilibria are given by the system of equations

$$\begin{aligned} x &= \frac{1}{1+k} \\ y &= \frac{\beta-(\beta+k)\varepsilon-\alpha-(\alpha\beta-\alpha)x}{\beta+k}. \end{aligned} \tag{4.2}$$

This gives, for $k=1$,

$$(x,y)=\left(\frac{1}{2},-\frac{1}{15}-\varepsilon\right), \tag{4.3}$$

and for $k=0$,

$$(x,y)=\left(1,\frac{1}{5}-\varepsilon\right). \tag{4.4}$$

The x locations of the equilibria are fixed, but the equilibria are located on the splitting manifold for

$$\varepsilon=\frac{1}{5} \tag{4.5}$$

and

$$\varepsilon=-\frac{1}{15}. \tag{4.6}$$

When

$$0<\varepsilon<\frac{1}{5},$$

solutions are attracted to a globally stable pseudoequilibrium. So, although the equilibrium boundary collision is interesting, it does not qualitatively change the dynamics of the system. Instead, the equilibrium escapes the splitting manifold and becomes a more classically recognizable, real equilibrium.

However, there is a fused focus Hopf bifurcation which occurs when $\varepsilon=0$. The stable Filippov equilibrium becomes unstable, giving rise to a stable periodic orbit. This makes the dynamics of the second border collision (4.6) more globally interesting.

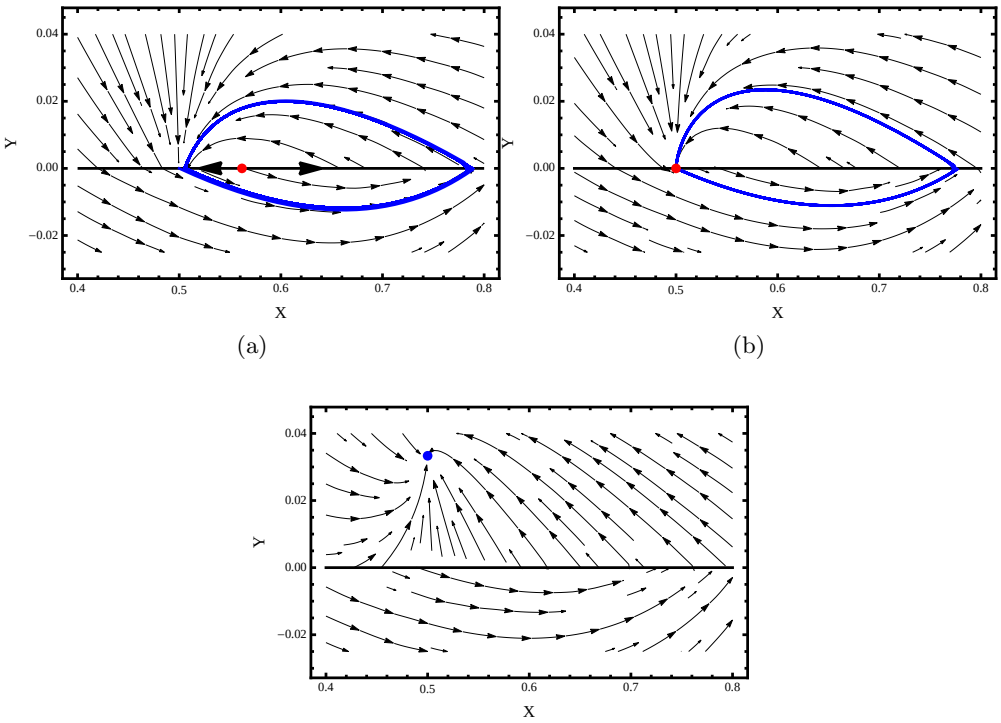

Figure 4.3: Global picture of the border collision bifurcation. (A) $\varepsilon = -1/17$, there exists one unstable pseudonode, with a large stable periodic orbit. (B) The bifurcation happens at $\varepsilon = -1/15$, and the periodic orbit becomes a homoclinic orbit. (C) $\varepsilon = -1/10$ and all solutions are attracted to a globally stable equililbrium.

For convenience we will define

$$\varepsilon_0 = -\frac{1}{15}. \tag{4.7}$$

In the interest of facilitating the discussion of the global bifurcation, we will look at the boundary collision in a nonstandard direction, as a pseudoequilibrium which becomes real when it escapes the splitting manifold through an endpoint of a sliding region. Figure 4.3 shows the border collision bifurcation. The following theorems address the existence and stability of the equilibrium and pseudoequilibrium as the system moves through the bifurcation.

Theorem 2. *For $\varepsilon_0 < \varepsilon < 0$, there exists a unique unstable pseudonode.*

Proof. Stability of the sliding region is given by

$$\frac{d}{d\lambda}(f \cdot \nabla h)|_{y=0} = \frac{d}{dk}(\beta - \beta\varepsilon - k\varepsilon - \alpha - (\beta + k)y - (\alpha\beta - \alpha)x)|_{y=0} = -\varepsilon.$$

So, for $\varepsilon < 0$, the sliding region is unstable. We must show that the sliding region contains a unique pseudoequilibrium, and that pseudoequilibrium is unstable. We first show that it is unique.

Pseudoequilibria are found on regions of the splitting manifold where the vector fields are colinear. This gives a condition on x and ε

$$-10\varepsilon - 3x + 5x\varepsilon + 4x^2 = 0. \tag{4.8}$$

So, we need to show that for $\varepsilon_0 < \varepsilon < 0$, there is only one solution to this equation inside the sliding region. This result can be clearly seen by plotting equation (4.8) and the bounds of the sliding region, as in Figure 4.4, however for the sake of rigor we prove uniqueness below.

We can rewrite equation (4.8) as follows

$$\varepsilon = \frac{4x^2 - 3x}{10 - 5x}, \tag{4.9}$$

noting that $x = 2$ was also not a valid solution in the original equation. The ε range $\varepsilon_0 < \varepsilon < 0$ corresponds to a range of x values,

$$\frac{1}{2} < x < \frac{3}{4}.$$

Therefore, because the only minimum of equation (4.9) occurs at

$$x = 2 - \frac{\sqrt{10}}{2}$$

and the asymptote occurs at $x = 2$, if the pseudoequilibrium exists, it is unique. To show that the pseudoequilibrium exists, we employ a change of perspective, which is possible only because the bounds of the sliding region are lines in (x, ε) space. First it is obvious that a solution to equation (4.9) exists for $\varepsilon \in (\varepsilon_0, 0)$. The boundaries of the

sliding region are given by lines in (x, ε) space,

$$x = \frac{3}{4} + \frac{15}{4}\varepsilon$$

and

$$x = \frac{3}{4} + \frac{5}{4}\varepsilon.$$

Writing these instead as ε bounds, we see that

$$\frac{3}{4} + \frac{15}{4}\varepsilon < x < \frac{3}{4} + \frac{5}{4}\varepsilon$$

if and only if

$$\frac{4}{5}x - \frac{3}{5} < \varepsilon < \frac{4}{15}x - \frac{1}{5}.$$

The following shows that

$$\frac{4x^2 - 3x}{10 - 5x} > \frac{4}{5}x - \frac{3}{5}.$$

This condition is true if and only if

$$(4x - 3)\left(\frac{x}{2 - x}\right) > 4x - 3$$

which, because $4x - 3 < 0$ in this x range, is equivalent to

$$\frac{x}{2 - x} < 1.$$

Because the function on the left side is monotonically increasing when $x < 2$, the maximum occurs when

$$x = \frac{3}{4}$$

and

$$\frac{x}{2 - x} = \frac{3}{5} < 1.$$

Additionally, we see that

$$\frac{4x^2 - 3x}{10 - 5x} < \frac{4}{15}x - \frac{1}{5},$$

which is equivalent to

$$\frac{x}{2-x} > \frac{1}{3}.$$

Now, the left function has a minimum at

$$x = \frac{1}{2},$$

where

$$\frac{x}{2-x} = \frac{1}{3},$$

proving the condition. Therefore, the ε given by equation (4.9) is in the correct bounds, so x is a pseudoequilibrium for the given ε.

We now show that the pseudoequilibrium is an unstable equilibrium of the sliding flow. The sliding flow is found by solving the system (3.3), and then using equation (3.4). In this system, $\lambda^*(x) = k^*(x)$, and the flow in the sliding region is given by

$$\dot{x} = 1 - x - k^*(x)x$$

The stability of the pseudoequilibrium is then given by the sign of the derivative of the right side of this equation, evaluated at the equilibrium. The derivative is

$$f'(x) = 1 - k^* - \left(\frac{dk^*}{dx}\right)x = \frac{-3 + 5\varepsilon + 8x}{-10\varepsilon}.$$

We've already seen that for these ε values, the pseudoequilibrium is bounded in x by

$$\frac{1}{2} < x < \frac{3}{4}.$$

This gives us a range on f',

$$\frac{1 + 5\varepsilon}{-10\varepsilon} < f'(\varepsilon) < \frac{3 + 5\varepsilon}{-10\varepsilon}.$$

Both the upper and lower bounds are positive for $\varepsilon_0 < \varepsilon < 0$, implying that the pseudoequilibrium is unstable. So, in this parameter range the pseudoequilibrium is totally unstable.

□

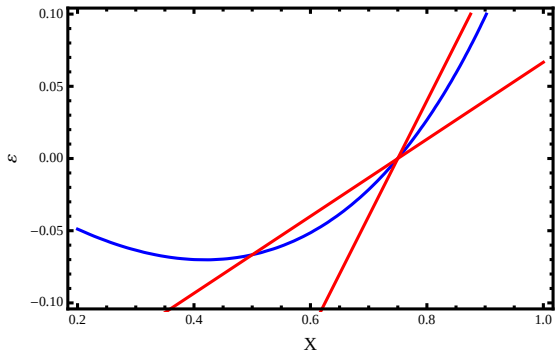

Figure 4.4: Indication of the existence and uniqueness of a pseudoequilibrium for the parameter range given in Theorem 2. The red lines are the boundaries of the sliding region, lines in (x, ε) space. The blue curve is the solution to (4.9). In the region where this solution is between the boundaries of the sliding region, a pseudoequilibrium exists.

Theorem 3. *For $\varepsilon < \varepsilon_0$, there exists one globally stable, real equilibrium, and no pseudoequilibria.*

Proof. First, the location of the equilibrium for the region $k = 1$ is given by (4.3), which shows that this equilibrium is real in the specified parameter range. The stability of the equilibrium is not dependent on ε, and has eigenvalues

$$\lambda = -2$$

and

$$\lambda = -\frac{3}{2},$$

indicating stability. the equilibrium for the region $k = 0$ remains virtual. So, it only remains to prove that there exist no pseudoequilibria in this range. This is done using the same method as in Theorem 2, and again analysis shows that for $\varepsilon < \varepsilon_0$, the ε given by equation (4.9) is outside the range of the sliding region. Specifically,

$$\frac{4x^2 - 3}{10 - 5x} > \frac{4}{15}x - \frac{1}{5}$$

for

$$x < \frac{1}{2},$$

which follows immediately from the calculation done in Theorem 2. So, no pseudoequilibrium exists in this parameter range.

□

The local dynamics at $\varepsilon = \varepsilon_0$, corresponding to the border collision, are unique to nonsmooth systems (See Figure 4.5). In the region $y > 0$, all trajectories converge to the equilibrium. The eigenvectors are both transverse to the splitting manifold, and do not depend on ε, or the location of the equilibrium. However, in the region $y < 0$, trajectories are repelled from the equilibrium, and are instead attracted to the virtual equilibrium of the $k = 0$ system. In the direction along the sliding region, the filippov flow takes solutions away from the equilibrium. So, the equilibrium has two unstable directions, one along the splitting manifold, given by the Filippov flow, and the other transverse to the manifold, with infinite repulsion. It is noteworthy that the location of the stable and unstable directions topologically disallow this situation in a smooth system.

However, this local picture is unsurprising in a nonsmooth system, and is in fact typical of a border collision. What may be surprising is the change in stability of the equilibrium as the system passes through the bifurcation, which is intimately tied to the angle between the splitting manifold and the vector field in the $k = 0$ region. This is because the vector field in the $k = 1$ region of space will always be in the direction of the equilibrium point, at an angle dependent on a ratio of the eigenvalues. The angle between the splitting manifold and the $k = 0$ vector field must be small enough for the convex combination to result in a vector pointing away from the equilibrium, along the manifold. In Welander's system, if the vector field in the $k = 0$ region were vertical, the equilibrium would not persist as a psuedoequilibrium, and the structure of the bifurcation would be uninteresting.

4.3.2 Global Bifurcation Structure in the Border Collision

The previous section discussed local dynamics as $\varepsilon = \varepsilon_0$, but the system also displays an interesting global bifurcation. The globally stable periodic orbit transitions to a globally stable equilibrium point, through a homoclinic implosion of sorts. The following theorems will explain this further.

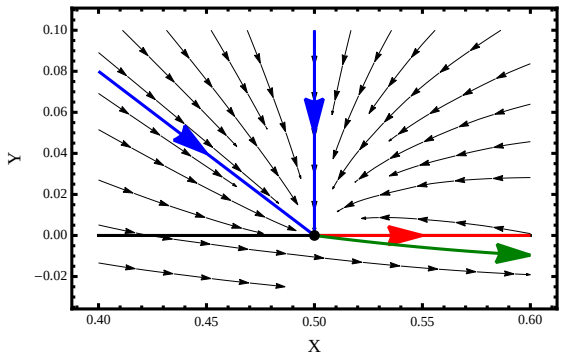

Figure 4.5: Local picture near the boundary equilibrium bifurcation. The blue arrows are stable solutions given by the eigenvectors of the $y = 0$ system. The red line is a sliding solution leaving hyperbolically from the boundary equilibrium. The green trajectory is the unique trajectory which leaves the boundary point in finite time.

Theorem 4. *For $\varepsilon_0 < \varepsilon < 0$, there exists a periodic orbit which intersects the line $y = 0$ with x value in the interval*

$$I = \left(\frac{1}{2}, \frac{3}{4} + \frac{15}{4}\varepsilon\right).$$

Proof. We consider the return map of trajectories from I to I, and show that the interval maps to a subset of itself. Then, the Brouwer Fixed Point Theorem immediately gives the existence of a periodic orbit. This is in fact very simple to show. First, we note that trajectories with initial values in this interval return to the line $y = 0$ in a bounded interval, with

$$x > \frac{3}{4}.$$

Moreover, all trajectories originating from the splitting manifold with

$$x > \frac{3}{4} + \frac{15}{4}\varepsilon$$

will intersect the splitting manifold again in I. This is a result of uniqueness of solutions in smooth dynamical systems, and a lack of invariant sets in the region $y > 0$. The argument is three fold. For

$$x > \frac{3}{4} + \frac{15}{4}\varepsilon,$$

and $\varepsilon_0 < \varepsilon < 0$,

$$f(x,0) \cdot \begin{pmatrix} 0 \\ 1 \end{pmatrix} > 0,$$

meaning the vector field points away from the splitting manifold, so trajectories can't return to the splitting manifold to the right of the interval. The system in $y > 0$ is also linear, and the equilibrium has a vertical eigenvector $\vec{v} = e_2$. This immediately shows the existence of a vertical trajectory along the line

$$x = \frac{1}{2},$$

converging to the virtual equilibrium. So, trajectories can't return to the splitting manifold to the left of the interval. However, solutions are easily seen to be bounded, and the lack of invariant sets in the region $y > 0$ indicates that solutions must return to the splitting manifold, indicating that the return map exists, and maps I to itself. So, there exists a periodic orbit intersecting the splitting manifold in this interval. □

One should note that this result immediately implies that the periodic orbit limits to an orbit through

$$x = \frac{1}{2}$$

as $\varepsilon \to \varepsilon_0$. This is in fact a homoclinic orbit coincident to the equilibrium border collision.

Theorem 5. *For $\varepsilon = \varepsilon_0$, there exists a homoclinic orbit through*

$$x = x_0 = \frac{1}{2}.$$

Proof. There is a unique trajectory emanating from the equilibrium point $(x_0, 0)$ into the region $y < 0$, based on the form of the $k = 0$ system. This trajectory crosses the splitting manifold at some point $x > 1$. All trajectories with initial condition $x > x_0$, $y > 0$ converge to the equilibrium point without crossing the splitting manifold, because of the following argument. Trajectories are not allowed to cross the splitting manifold at any point $x > x_0$, because in that region, $\dot{y} > 0$ along $y = 0$. Moreover, trajectories can't cross the splitting manifold anywhere where $x < x_0$, because there exists a vertical

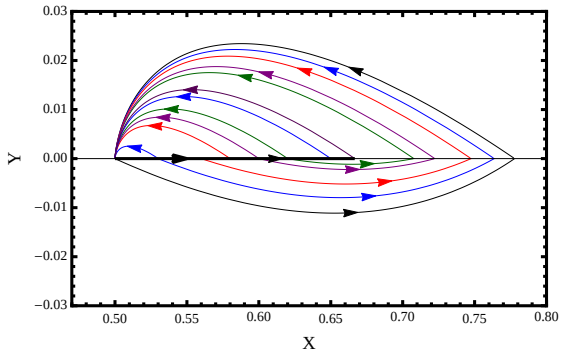

Figure 4.6: The global picture at the boundary collision bifurcation. The thick black line is the sliding solution, from which trajectories leave arbitrarily in either direction. Inside the black homoclinic orbit there is a continuum of homoclinic orbits.

line trajectory along $x = x_0$. Therefore, trajectories are squeezed from either side, and in particular the unique trajectory in the $k = 0$ region, with initial condition $x = x_0$ must then return to $x = x_0$ after an infinite period, giving a homoclinic orbit. □

Theorem 6. *Using Filippov dynamics, when $\varepsilon = \varepsilon_0$ all orbits which slide along the splitting manifold are homoclinic orbits.*

Proof. First, because all trajectories in the $y > 0$, $x > x_0$ region of phase space converge to the boundary equilibrium, it is clear that trajectories which travel arbitrarily along the sliding region and then escape to this region of phase space are homoclinic orbits. If an orbit leaves the splitting manifold into the $y < 0$ region, it is constrained by the homoclinic orbit described in Theorem 5. Because there are no invariant sets in this region, these orbits will cross the splitting manifold, and then converge to the boundary equilibrium, and hence are also homoclinic orbits. See Figure 4.6 for an illustration of these orbits.

□

So, we've shown that Welander's nonsmooth model contains a fused focus bifurcation, analogous to a supercritical Hopf bifurcation. Additionally, we see border collision bifurcation, concurrent with a continuum of homoclinic orbits. In Chapters 6 and 7 we compare these nonsmooth phenomena with the corresponding bifurcations in Welander's smooth model, but first we discuss this problem more generally.

Chapter 5

The Relationship Between Smooth and Nonsmooth Systems

Welander makes an implicit assumption in his paper that using a nonsmooth system simplifies the analysis of the system. At first glance this assumption seems justified, as the system on either side of the discontinuity is linear. However, this also raises an extremely important question pertaining to the relationship between the smooth and nonsmooth system. Such an approach would be justified if one knew that the nonsmooth system and smooth system behaved qualitatively in the same way, but that assumption is not necessarily mathematically justified. This chapter will address a few aspects of this issue.

5.1 Nonlinear Sliding

Nonsmooth systems are often the result of a pointwise convergence of a smooth system to a nonsmooth, for instance in Welander's model, where

$$k = \frac{1}{\pi}\tan^{-1}\left(\frac{y}{a}\right) + \frac{1}{2} \to \begin{cases} 1 & y > 0 \\ 0 & y < 0 \end{cases}$$

as $a \to 0$. But, when attempting to infer the behavior of the smooth system by looking at the limiting nonsmooth system, Jeffrey has shown that one is unable to conclude

anything qualitative about the smooth system [16, 17]. This is because of a phenomenon he calls *nonlinear sliding*. The name *nonlinear sliding* is due to the addition of nonlinear terms in λ to the vector field, but which are nonzero only on the splitting manifold. Consider the following example system

$$\begin{pmatrix} \dot{x} \\ \dot{y} \end{pmatrix} = \begin{pmatrix} 1 \\ 3 - \lambda - x \end{pmatrix} + (\lambda - \lambda^2) \begin{pmatrix} 1 \\ 1 \end{pmatrix}$$

where λ is as in (3.2), and $h = y$. In Filippov's convex combination method, as discussed in Chpater 3, the nonlinear terms do not affect the sliding dynamics, as the only relevant information is the smooth vector fields $f_0(x)$ and $f_1(x)$. In this case, some simple analysis finds an attracting sliding region, occurring between the tangencies $x = 2$ and $x = 3$. However, the only stipulation needed in finding sliding solutions is that the system (3.3) is solvable for $\lambda \in [0, 1]$. Using this, we solve the equation

$$3 - x - \lambda^2 = 0$$

and find that a solution exists in the proper range for $x \in [1, 3]$. This is still a unique attracting sliding solution, but it extends into a Filippov crossing region. Additionally, for other vector fields, more complicated dynamics can exist on the splitting manifold, including folds [17]. This behavior is not captured by Filippov's method.

It is reasonable to wonder whether this is all simply a mathematical artifact, with no basis in real behavior. However this is not the case. Actually, these nonlinear terms can arise naturally from nonmonotonic transition functions, which converge pointwise to the same piecewise smooth limit. For instance, using the nonmonotonic transition function

$$F(x) = \frac{1}{2} + \frac{1}{2}\left(s + s(1 - s^2)\right),$$

with s a monotonic function converging to λ as some steepness parameter approaches 0, gives smooth trajectories which limit to nonlinear sliding trajectories.

Because infinitely many different functions can limit to the same nonsmooth function, there are infinitely many possible nonlinear sliding solutions that are not captured by a Filippov analysis. This spells trouble for nonsmooth analysis as a stand in for smooth analysis, however there are some cases for which some understanding can be

gained. A main result of this thesis is the use of a *blow up* system to compare the fused focus of Welander's model to a standard supercritical Hopf bifurcation. However, we will first discuss briefly a different method used to compare smooth and nonsmooth systems, called regularization.

5.2 Regularization

Regularization is a way of smoothing out nonsmooth systems, and is a standard method first popularized by Sotomayor and Teixeira [21, 22, 23, 24, 25]. The regularization method has not answered all of the questions inherent in analyzing the relationship between smooth and nonsmooth systems, but it has set out some conditions for when the smoothing contains solutions analogous to Filippov sliding solutions. In the regularization method, a C^∞ transition function is defined to smooth the system in a region around the splitting manifold, which is here assumed to be the hyperplane $x_1 = 0$.

$$\phi(x_1) = \begin{cases} 1 & x_1 \geq 1 \\ 0 & x_1 \leq -1 \end{cases} \tag{5.1}$$

with $\phi'(x_1) > 0$ when $x_1 \in (-1, 1)$. This function is not given explicitly, but does exist. Then, define

$$\phi_\varepsilon(x_1) = \phi\left(\frac{x_1}{\varepsilon}\right), \tag{5.2}$$

and the regularized vector field

$$f_\varepsilon(x) = \phi_\varepsilon(x_1) f_1(x) + (1 - \phi_\varepsilon(x_1))\, f_0(x). \tag{5.3}$$

This gives a family of vector fields depending on ε, each of which agree exactly with the nonsmooth system outside a strip of width 2ε around the splitting manifold. Inside the ε strip, the regularized vector fields are a smooth approximation to the nonsmooth transition.

Using the regularization method, one can then use a coordinate change to transform the system into a fast-slow system, and use geometric singular perturbation theory to analyze the result. The coordinate change is called the *polar blow up*, and is given in

two dimensions by

$$\begin{aligned} x &= \eta \cos\psi \\ \varepsilon &= \eta \sin\psi \end{aligned} \tag{5.4}$$

From this coordinate change, we consider a new system

$$\begin{aligned} \eta\dot{\psi} &= \alpha_1(\eta, \psi, y) \\ \dot{y} &= \alpha_2(\eta, \psi, y), \end{aligned} \tag{5.5}$$

where we wish to perturb away from $\eta = 0$ corresponding to a perturbation from $\varepsilon = 0$. It has been shown that in the coordinate changed system, the critical manifold corresponds exactly to the sliding solutions of the Filippov vector field, and the stability of the manifold is the same as the stability of the sliding region [23, 22].

The regularization method has been used to apply smooth techniques to nonsmooth systems, as in [21]. However, there are some mathematical questions which are outside the purview of this technique. Regularization assumes that the Filippov method fully describes the dynamics of the nonsmooth system, and hence will always replicate the Filippov dynamics. It is incapable of describing an arbitrary smooth system which limits pointwise to the nonsmooth system, like a system which displays nonlinear sliding, as the monotonicity condition on ϕ is necessary to the results. Moreover, it does not apply to many relevant systems, because the transition function ϕ must achieve the values 0 and 1 away from the edges of the space. For instance, in Welander's system, the transition function is an inverse tangent, which only approaches 0 and 1 at $\pm\infty$. The use of a ϕ which exists but remains unspecified is rather impractical, and limits the relevance of the technique to applications. And finally, it is philosophically clear that regularization is fundamentally incapable of answering any question about a previously given smooth system, for which analysis is simplified using a nonsmooth limit. This is due to the somewhat arbitrary smoothing necessary to the technique, which is usually not clearly equivalent to the original smooth system. Results in regularization theory give the existence of a smoothing for which the nonsmooth phenomena are replicated in the resulting system, but cannot allow you to conclude that the originally given system also contains a similar phenomena. For these reasons, the regularization technique is limited, and is incapable of answering the question raised by Welander's system, namely whether the nonsmooth phenomena are also present in the smooth system. To

answer this question for the fused focus bifurcation, we use a different blow up method, described in the next chapter. The relationship between the border collision and the corresponding phenomenon in the smooth system will be discussed in Chapter 7.

Chapter 6

Perturbation of the Fused Focus Bifurcation

The previous chapter has illuminated some problems inherent in the comparison of smooth and nonsmooth systems. Regularization, described in Section 5.2, is the most widely accepted method of perturbing a nonsmooth system into a smooth system, but this method creates an arbitrary smooth system guaranteed to agree with the Filippov analysis. Perhaps more alarmingly, Jeffrey's work in nonlinear sliding phenomena has shown that one can generally not expect a perturbed smooth system to display Filippov dynamics, and in fact there are infinitely many different scenarios which can be seen in nearby smooth systems, as described in Section 5.1. However, in many applications, including Welander's model, a nonsmooth limit is used to simplify the analysis of the system, and it is important to understand the relationship between the given smooth system and the nonsmooth limit. In Welander's model, we can avoid these complications because we are given the smooth system in addition to the limiting nonsmooth system. Therefore, regularization techniques are unnecessary, and we can rigorously answer this question about Welander's smooth model. First we discuss the perturbation of the fused focus bifurcation, using a coordinate change to create the *blow up system*, described in detail in Section 6.1.

6.1 Blow Up Method

Because the fused focus bifurcation in Welander's system occurs along the splitting manifold $y = 0$, in the regular Filippov system it is impossible to do any standard analysis. So, it is useful to do a coordinate change to instead look at the system in terms of independent variables x and k. We call this the *blow up system*, because it is effectively zooming in on the behavior of the system near $y = 0$. It should be explicitly noted that this is different from the blow up methods of Sotomayor-Teixera regularization, in which the system is smoothed in a size δ region around the splitting manifold. Instead, this coordinate changed system is equivalent to the original system, as long as the smoothness parameter $a \neq 0$. The method of using a coordinate change to transform a singularity into a regular point has been used in several other mathematical areas, notably celestial mechanics [26].

Here, using (2.4), if

$$z = \frac{y}{a},$$

we see that

$$k = \Phi(z) = \frac{1}{\pi}\tan^{-1}(z) + \frac{1}{2}. \tag{6.1}$$

The chain rule tells us

$$\dot{k} = \frac{d\Phi}{dz}\frac{dz}{dy}\frac{dy}{dt} = \frac{1}{a}\Phi'\left(\Phi^{-1}(k)\right)\left(\beta - \beta\varepsilon - k\varepsilon - \alpha - a(\beta + k)\Phi^{-1}(k) - (\alpha\beta - \alpha)x\right).$$

For the k as defined,

$$\Phi^{-1}(k) = \tan\left(\pi(k - \frac{1}{2})\right) = -\cot(\pi k)$$

and

$$\Phi'(y) = \frac{1}{\pi}\frac{1}{1 + z^2}.$$

Therefore the blow up system in terms of x and k is

$$\begin{aligned} \dot{x} &= 1 - x - kx \\ \dot{k} &= \frac{1}{a\pi}\sin^2(\pi k)\left(\beta - \beta\varepsilon - k\varepsilon - \alpha + a(\beta + k)\left(\cot(\pi k)\right) - (\alpha\beta - \alpha)x\right) \end{aligned} \tag{6.2}$$

There are a few important things to note about this system. First, for all $a \neq 0$ it is equivalent to the original system. The places where difficulties arise are where the function Φ is not invertible, at $k = 0$ and $k = 1$. The derivative $\Phi'(z)$ is bounded everywhere, as the dependence on the parameter a has been removed by the coordinate change. Therefore, this system is well defined and smooth everywhere away from the k-boundaries. Because a is a small parameter, (6.2) is a fast slow system. k is the fast variable and x is the slow variable. We can do a change of time scale to get the fast system.

$$\begin{aligned} x' &= a\,(1 - x - kx) \\ k' &= \frac{1}{\pi}\sin^2(\pi k)\,(\beta - \beta\varepsilon - k\varepsilon - \alpha + (\beta + k)\,(a\cot(\pi k)) - (\alpha\beta - \alpha)x) \end{aligned} \tag{6.3}$$

An equilibrium of the Filippov flow exists under the condition that the system of equations

$$\begin{gathered} \beta - \beta\varepsilon - k\varepsilon - \alpha - (\alpha\beta - \alpha)x = 0 \\ 1 - x - kx = 0 \end{gathered}$$

is solvable for a $k \in [0, 1]$. For ε near $\varepsilon = 0$, the bifurcation point, this system is solvable, although for $|\varepsilon|$ sufficiently large, this pseudoequilibrium disappears. This disappearance is related to the border collision bifurcation, which is discussed in Section 4.3.

We will show that the fused focus bifurcation is a limit of a smooth supercritical Hopf bifurcation, but first we prove two lemmas.

Lemma 7. *The Filippov equilibrium perturbs to a unique smooth equilibrium.*

Proof. Showing that the Filippov equilibrium perturbs to the smooth equilibrium is a singular perturbation problem if one uses the blow up system (6.3) and (6.2). For an introduction to geometric singular perturbation theory, or GSPT, the reader is referred to the work of Jones [27].

Because a is a small parameter, the blow up system is fast slow, with k being the fast variable and x being the slow variable, and one can analyze this system using GSPT techniques. The system gives a critical manifold of

$$\beta - \beta\varepsilon - k\varepsilon - \alpha - (\alpha\beta - \alpha)x = 0.$$

An equilibrium is a point on this critical manifold for which

$$x = \frac{1}{1+k}.$$

These are also exactly the conditions for a Filippov equilibrium in the nonsmooth (x, y) system. As long as $\varepsilon \neq 0$, this critical manifold is immediately seen to be normally hyperbolic, so singular perturbation theory gives the existence for small $a > 0$ of a unique equilibrium in the neighborhood of the Filippov equilibrium. To show that the equilibrium in the smooth system exists and is unique, we apply the Intermediate Value Theorem, and show monotonicity of the equilibrium function. Using (2.2) and (2.4), we can calculate equilibria in terms of ρ. Letting $k_* = k(\rho_*)$ be the k value at the equilibrium ρ_*, we get

$$T_* = \frac{1}{1+k_*}$$
$$S_* = \frac{\beta}{\beta+k_*}.$$

Then, because $\rho_* = -\alpha T_* + S_*$, the equilibria are solutions to the equation

$$-\frac{\alpha}{1+k_*} + \frac{\beta}{\beta+k_*} = \rho_* \tag{6.4}$$

or

$$f(\rho) = -\frac{\alpha}{1+k_*} + \frac{\beta}{\beta+k_*} - \rho_* = 0 \tag{6.5}$$

The Intermediate Value Theorem gives us the existence of a root of $f(\rho)$ (the function is smooth, as long as $a \neq 0$). Because $k > 0$, the fractional terms are bounded, so when $k \to 1$, $\rho \to +\infty$, and $f(\rho) \to -\infty$, and when $k \to 0$, $\rho \to -\infty$ and $f(\rho) \to +\infty$. Showing that the function is monotone gives us the uniqueness of the root.

$$\frac{\partial f(\rho)}{\partial \rho} = \frac{\partial k}{\partial \rho}\left(\frac{\alpha}{(1+k)^2} - \frac{\beta}{(\beta+k)^2}\right) - 1.$$

Both fractional terms are positive, because $\alpha > 0$ and $\beta > 0$. We show that

$$\frac{\beta}{(\beta+k)^2} > \frac{\alpha}{(1+k)^2}.$$

Then, because

$$\frac{\partial k}{\partial \rho} > 0,$$

$$\frac{\partial f(\rho)}{\partial \rho} < 0,$$

so the function is monotone and the root is unique. We check the condition first for $k = 0$. Then, the condition is

$$\frac{1}{\beta} > \alpha,$$

or, plugging in α and β, $2 > 0.8$. We then solve the equation

$$\frac{\beta}{(\beta + k)^2} - \frac{\alpha}{(1 + k)^2} = 0.$$

Using the quadratic formula to solve for k, we get

$$k = \frac{-2\beta(1 - \alpha) \pm \sqrt{4\alpha\beta(\beta - 1)^2}}{2(\beta - \alpha)}$$

This gives two solutions for k, given our parameters α and β. These solutions are

$$k = \frac{1 \pm \sqrt{10}}{3},$$

both of which are outside the range $0 < k < 1$. So,

$$\frac{\alpha}{(1 + k)^2} - \frac{\beta}{(\beta + k)^2} < 0,$$

and $f(\rho)$ is monotone. Thus, the root is unique. Therefore, the Filippov equilibrium perturbs to the unique smooth equilibrium. The stability of the equilibrium changes when ε goes through 0. □

Lemma 8. *As $a, \varepsilon \to 0$, the equilibrium approaches the point*

$$(x, k, \varepsilon, a) = \left(\frac{3}{4}, \frac{1}{3}, 0, 0\right). \tag{6.6}$$

Proof. GSPT breaks down when $\varepsilon = 0$, because the critical manifold is no longer normally hyperbolic. In fact, the blow up system gives a line of equilibria, along

$$x = \frac{3}{4}.$$

This is expected, as the bifurcation point is also only center stable. However, the blow up system gives a unique candidate for a point around which to analyze the system. This is the intersection of the vertical line

$$x = \frac{3}{4}$$

and the nullcline

$$x = \frac{1}{1+k},$$

which gives the relevant point

$$(x, k, \varepsilon, a) = \left(\frac{3}{4}, \frac{1}{3}, 0, 0\right).$$

Because the system is smooth away from $k = 0$ and $k = 1$, the equilibrium will limit to this point as $a \to 0$ and $\varepsilon \to 0$. It should be noted that this is a two dimensional limit, so generally having independent limits as these parameters approach zero is not good enough. However, the smoothness of the system allows this conclusion. □

Theorem 9. *The fused focus bifurcation perturbs to a smooth supercritical Hopf bifurcation as $a > 0$.*

Proof. The blow up system

$$\begin{aligned} x' &= a(1 - x - kx) \\ k' &= \frac{1}{\pi}\sin^2(\pi k)\left(\beta - \beta\varepsilon - k\varepsilon - \alpha + (\beta + k)\left(a\cot(\pi k)\right) - (\alpha\beta - \alpha)x\right), \end{aligned} \tag{6.7}$$

is smooth for all values of a, including $a = 0$ (staying away from $k = 0, k = 1$). Therefore a more standard stability analysis of the relevant point (6.6) is possible.

To use a Taylor series expansion of the system to analyze the nearby behavior, let

$$\xi = x - \frac{3}{4},$$

and

$$\psi = k - \frac{1}{3}.$$

The expansion of $f_1 = a(1 - x - kx)$ around the point is straightforward, and yields

$$\dot{\xi} = -\frac{4}{3}a\xi - \frac{3}{4}a\psi. \tag{6.8}$$

The expansion of the $\dot{k}$ equation is more complicated because of the number of terms, but calculation shows that the Taylor expansion is

$$\dot{\psi} = -\frac{5}{8\pi}\varepsilon + \frac{5}{8\pi\sqrt{3}}a + \frac{3}{10\pi}\xi + \left(\frac{\sqrt{3}}{4\pi} - \frac{5}{12}\right)a\psi - \left(\frac{5}{4\sqrt{3}} + \frac{3}{4\pi}\right)\varepsilon\psi + \frac{\sqrt{3}}{5}\xi\psi + \mathcal{O}(3). \tag{6.9}$$

The Jacobian of the system of equations, using the expansion, is

$$J = \begin{bmatrix} -\frac{4}{3}a & -\frac{3}{4}a \\ c_1 & c_3\varepsilon + c_4 a \end{bmatrix} = \begin{bmatrix} -\frac{4}{3}a & -\frac{3}{4}a \\ \frac{3}{10\pi} & -\left(\frac{5}{4\sqrt{3}} + \frac{3}{4\pi}\right)\varepsilon + \left(-\frac{5}{12} + \frac{\sqrt{3}}{4\pi}\right)a \end{bmatrix}. \tag{6.10}$$

This is singular when $a = \varepsilon = 0$. A calculation of the trace and discriminant of this Jacobian indicates the existence of a Hopf bifurcation in a neighboorhood of the singular point $a = \varepsilon = 0$. The trace of the jacobian is

$$\text{tr} = \left(\frac{-21}{12} + \frac{\sqrt{3}}{4\pi}\right)a - \left(\frac{5}{4\sqrt{3}} + \frac{3}{4\pi}\right)\varepsilon,$$

and so the trace is zero along a line in (ε, a) space, limiting to the fused focus. The following tedious but necessary calculation shows that the genericity condition holds. All of this is done with the Taylor expansion equations (6.8) and (6.9), included here

with more terms:

$$\begin{aligned}
\dot{\xi} &= -\tfrac{4}{3}a\xi - \tfrac{3}{4}a\psi \\
\dot{\psi} &= -\frac{5}{8\pi}\varepsilon + \frac{5}{8\pi\sqrt{3}}a + \frac{3}{10\pi}\xi + \left(\frac{\sqrt{3}}{4\pi} - \frac{5}{12}\right)a\psi - \left(\frac{5}{4\sqrt{3}} + \frac{3}{4\pi}\right)\varepsilon\psi + \frac{\sqrt{3}}{5}\xi\psi \\
&\quad + \left(-\frac{\sqrt{3}}{2} + \frac{5\pi}{12}\right)\varepsilon\psi^2 + \left(\frac{\pi}{2} + \frac{5\pi^2}{6\sqrt{3}}\right)\varepsilon\psi^3 + \left(\frac{\pi^2}{\sqrt{3}} - \frac{5\pi^3}{36}\right)\varepsilon\psi^4 \\
&\quad \left(-\frac{1}{2} - \frac{5\pi}{4\sqrt{3}}\right)a\psi^2 + \left(-\frac{\sqrt{3}\pi}{2} + \frac{5\pi^2}{18}\right)a\psi^3 + \left(\frac{\pi^2}{3} + \frac{5\pi^3}{12\sqrt{3}}\right)a\psi^4 \\
&\quad -\frac{\pi}{5}\xi\psi^2 + \frac{2\pi^2}{5\sqrt{3}}\xi\psi^3 + \frac{\pi^3}{15}\xi\psi^4 + \mathcal{O}(5)
\end{aligned}$$

The nondegeneracy condition is

$$b = \frac{1}{16}\left(f_{xxx} + f_{xyy} + g_{xxy} + g_{yyy}\right) + \frac{1}{16\omega}\left(f_{xy}\left(f_{xx} + f_{yy}\right) - g_{xy}\left(g_{xx} + g_{yy}\right) - f_{xx}g_{xx} + f_{yy}g_{yy}\right) \neq 0,$$

where ω is the imaginary part of the eigenvalue at the bifurcation point. Here $x = \xi$ and $y = \psi$, and f is the right side of the top equation, g is the right side of the bottom equation. All derivatives in b are calculated at the bifurcation point. It is immediately clear that all the f derivatives in b are 0.

$$g_{xx} = 0$$

$$g_{xy} = \frac{\sqrt{3}}{5}$$

$$g_{yy} = 2a\left(-\frac{1}{2} - \frac{5\pi}{4\sqrt{3}}\right)$$

$$g_{yyy} = a\left(-\frac{\sqrt{3}\pi}{2} + \frac{5\pi^2}{18}\right)$$

$$b = \frac{1}{16}\left(-3\sqrt{3}\pi a + \frac{5\pi^2 a}{3} + \frac{a\sqrt{3}}{5\omega} + \frac{\pi a}{2\omega}\right)$$

$$\omega = 675a^2 + 3025a^2\pi^2 + 1650\sqrt{3}a^2\pi - 3240a\pi$$

Given that $a \neq 0$, $\omega \neq 0$, and the genericity condition reduces to

$$-3\sqrt{3}\pi\omega + \frac{5\pi^2\omega}{3} + \frac{\sqrt{3}}{5} + \frac{\pi}{2} \neq 0$$

when a is small, ω is a very small negative number, so this term is in fact nonzero. We can also use the fact that ω is small and negative to see that $b < 0$. To show that the bifurcation is supercritical, we also need to find

$$d = \left.\frac{\partial \alpha}{\partial \varepsilon}\right|_{\varepsilon=0},$$

where α is the real part of the eigenvalue.

$$\alpha = \frac{1}{120\pi}\left(15\sqrt{3}a - 45\varepsilon - 105a\pi - 25\sqrt{3}\pi\varepsilon\right).$$

We see that d is negative. Because $b, d < 0$, we can conclude from the Hopf theorem that the equilibrium is stable for $\varepsilon > 0$, and unstable for $\varepsilon < 0$. Periodic orbits exist when $\varepsilon < 0$, and these periodic orbits are stable. Hence, the bifurcation is supercritical. The bifurcation occurs along a line in (ε, a) parameter space,

$$\left(\frac{-21}{12} + \frac{\sqrt{3}}{4\pi}\right)a - \left(\frac{5}{4\sqrt{3}} + \frac{3}{4\pi}\right)\varepsilon = 0.$$

To the right of this line, the equilibrium point is stable, and to the left the equilibrium point becomes unstable, and a small stable periodic orbit forms from a supercritical Hopf bifurcation. As $a \to 0$, the bifurcation line limits to the point $(\varepsilon, a) = (0, 0)$ in parameter space, showing that the supercritical Hopf bifurcation point limits to the nonsmooth fused focus bifurcation point as $a \to 0$ (see Figure 6.1). It should be reiterated that the coordinate change given in equation (6.3) is critical to this analysis, as the fused focus bifurcation here occurs in a smooth region of phase space. This allows the Taylor expansion and pointwise limit of the supercritical Hopf bifurcation.

□

An astute reader may notice that the Jacobian in (6.10) has a double zero eigenvalue at the nonsmooth bifurcation point. This might indicate that we should expect

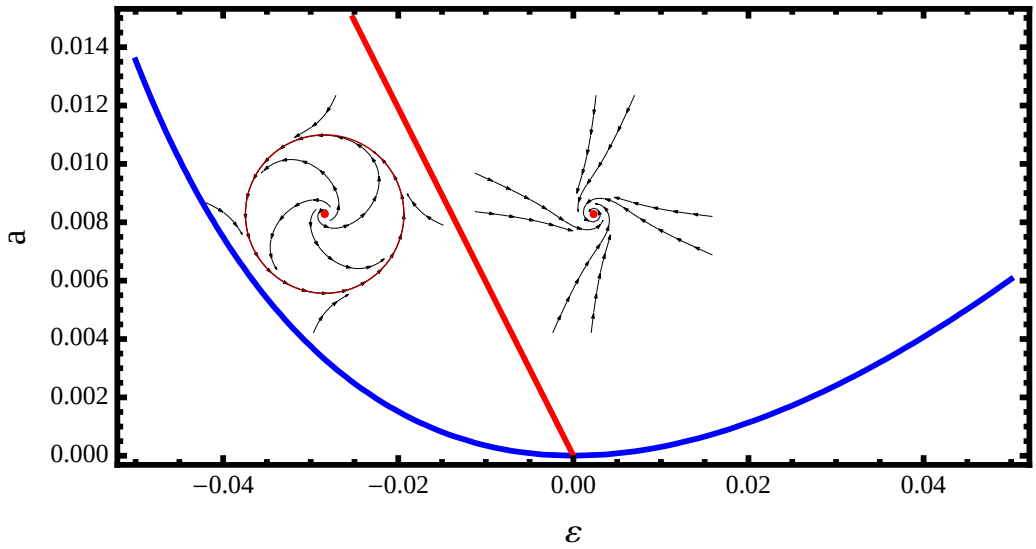

Figure 6.1: A plot of the trace (red) and discriminant (blue) of the Jacobian matrix. The smooth Hopf bifurcation occurs along the red curve, and limits to the nonsmooth bifurcation point.

a Takens-Bogdanov bifurcation structure, instead of a simple supercritical Hopf bifurcation. However, this does not occur here because the parameter region $a < 0$ is not allowed by the system, or, if one chooses to include it, one forces an extra symmetry as a negative sign in the inverse tangent in (2.4). In the smooth system, when $a > 0$, the periodic orbit which is formed by the Hopf bifurcation is later destroyed in a different bifurcation, which limits to the border collision bifurcation as $a \to 0$. This will be discussed in the next chpater.

So, the fused focus bifurcation in Welander's nonsmooth model is a direct extension of a smooth supercritical Hopf bifurcation.

Chapter 7

Perturbation of the Border Collision

The blow up method used in Chapter 6 unfortunately can't be used to analyze the border collision bifurcation. In the blow up system, the border collision occurs at the edge of the space, where $k = 1$, and so the coordinate change does not allow us to apply known analysis techniques for smooth systems. However, because we are given the smooth system for which the nonsmooth system is a limiting case, we can discuss the smooth version of the bifurcation directly. There are several key differences between this nonsmooth homoclinic bifurcation and a standard homoclinic bifurcation, which indicate that this phenomenon is not a limit of a smooth homoclinic bifurcation. The bifurcation does not leave behind a saddle equilibrium point. The homoclinic orbits are space filling. Most importantly, there is a shear in the stable and unstable directions of the equilibrium on the homoclinic orbit. We can also note that there are notable similarities in the system to a Takens Bogdanov bifurcation. If one looks at the entire bifurcation structure of the nonsmooth system, we see both a Hopf bifurcation and a homoclinic bifurcation. However, these bifurcations are separated in parameter space, with no opportunity to converge. We also do not see any saddle equilibria, or saddle node bifurcations, indicating that the nonsmooth system might not be a result of a Takens Bogdanov bifurcation. There are also some similarities to canard orbits. The homoclinic orbits are of all sizes, as if there is a canard explosion occurring at a single point.

Moreover, the aftermath of the nonsmooth bifurcation is attraction to a larger periodic structure, analogous to a relaxation oscillation. However, the model doesn't have the bistability inherent to canard systems. So, one wonders which smooth phenomena might limit to this nonsmooth homoclinic bifurcation. We use (2.4) to answer this question. Proving that the smooth phenomena limit to the homoclinic bifurcation is nontrivial, however simulations indicate that this is the case.

Theorem 10. *The real equilibrium which exists in the nonsmooth system for parameter ranges*

$$\varepsilon \in \left(-\infty, -\frac{1}{15}\right) \cup \left(\frac{1}{5}, \infty\right)$$

perturbs to the unique equilibrium of the smooth system as $a > 0$.

Proof. In this case, the analysis is easier if we use the nondimensionalized system (2.2). Real equilibria in the nonsmooth system are found by solving

$$T = \frac{1}{1+k}$$
$$S = \frac{\beta}{\beta+k}$$

for $k = 0, 1$, and then checking that $\rho = -\alpha T + S < \varepsilon$ or $\rho = -\alpha T + S > \varepsilon$, depending on the region. When $k = 1$,

$$\rho = \frac{-\alpha}{2} + \frac{\beta}{\beta+1} = -\frac{1}{15}$$

for the given parameters of α and β. When $k = 0$,

$$\rho = -\alpha + 1 = \frac{1}{5}.$$

The argument is the same for both cases where the equilibrium is real in the nonsmooth case, so we will consider the case where

$$\rho = \rho_0 = -\frac{1}{15}.$$

For this equilibrium to be real when $a = 0$, we must have

$$\varepsilon < -\frac{1}{15},$$

which is consistent with previous results. The value of the smooth equilibrium is given by solving the equation

$$-\frac{\alpha}{1+k} + \frac{\beta}{\beta+k} - \rho = f(\rho, a)$$

for ρ, where k is the smooth function given by (2.4). We use the Implicit Function Theorem. Because

$$\varepsilon < -\frac{1}{15},$$

which is the necessary and sufficient condition for

$$\rho_0 = -\frac{1}{15}$$

to be the globally stable equilibrium, there is a ball $\mathcal{B}(\rho_0, r)$ in which $\rho \neq \varepsilon$. In this ball,

$$\frac{\partial f}{\partial a} = \frac{\partial k}{\partial a}\left(\frac{\alpha}{(1+k)^2} - \frac{\beta}{(\beta+k)^2}\right).$$

$$\frac{\partial k}{\partial a} = -\frac{\rho - \varepsilon}{a^2 + (\rho-\varepsilon)^2} \neq 0,$$

because $\rho \neq \varepsilon$ anywhere in the ball around ρ_0. The other terms in the partial derivative are both positive, and don't cancel each other near $k = 1$, so

$$\frac{\partial f}{\partial a} \neq 0$$

in the ball around ρ_0. Therefore, there is a function $\rho = g(a)$ along which $f(\rho, a) = 0$. This shows that the equilibrium limits to the global equilibrium in the nonsmooth system, as long as the equilibrium doesn't fall on the splitting manifold. □

However, the periodic orbit seen in the nonsmooth system does not perturb to a unique periodic orbit as $a > 0$. Instead, the global behavior of the smooth system is fundamentally different from the global behavior in the nonsmooth system. The smooth system contains a supercritical Hopf bifurcation which is a direct analogue to a similar

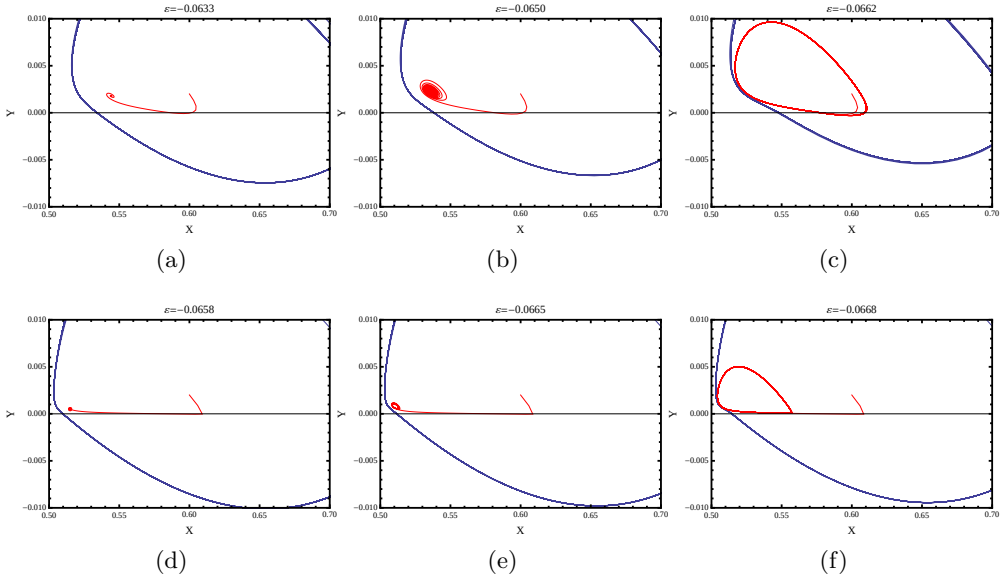

Figure 7.1: Numerical solutions to Welander's smooth model near the border collision bifurcation. the blue curve is a trajectory converging to the stable periodic orbit. The red curves are trajectories converging in backward time, either to an unstable equilibrium or an unstable periodic orbit. As ε decreases (right) the system undergoes a subcritical Hopf bifurcation, followed by a periodic orbit saddle node. As $a \to 0$ (down) the subcritical Hopf bifurcation and periodic orbit saddle node limit to the same point in parameter space. The squeezing seen in (C) and (F) is a smooth remnant of the homoclinic continuum in the nonsmooth model.

phenomenon in the nonsmooth system, as previously seen. However, the smooth system also contains a subcritical Hopf bifurcation in the parameter vicinity of $\varepsilon = \varepsilon_0$. The stable and unstable periodic orbits from these bifurcations grow until they annihilate each other in a periodic orbit saddle node bifurcation, leaving behind a globally stable equilibrium point. The subcritical Hopf bifurcation and the periodic orbit saddle node limit to the same parameter value as $a \to 0$, and the system becomes nonsmooth. This has serious implications for the relationship between smooth and nonsmooth systems. It implies that the homoclinic explosion is a fundamentally nonsmooth bifurcation. This is also indicated by the inadequacy of the blow up method in analyzing this bifurcation. It is likely that the relationship between the border collision and the smooth bifurcation is a cross section of a higher codimension bifurcation structure including the parameters

α and β. Further bifurcation analysis is necessary to clarify that idea. However, at the very least this is strong evidence that nonsmooth systems may display fundamentally different behavior to smooth systems.

Moreover, the qualitative difference between the border collision and the corresponding smooth bifurcation is not a result of any nonlinear sliding phenomena influencing the structure.

Theorem 11. *The Welander nonsmooth system does not exhibit nonlinear sliding.*

Proof. We start with the blow up system defined in (6.2) and (6.3). As $a \to 0$, (6.3) zooms in on the behavior on the splitting manifold. Sliding solutions in the nonsmooth system are seen in this system as k nullclines that exist for $0 < k < 1$, i.e. places where solutions travel into the discontinuity boundary and remain. Letting $a = 0$, these nullclines are solutions to $k' = 0$, or

$$\beta - \beta\varepsilon - k\varepsilon - \alpha - (\alpha\beta - \alpha)x = 0.$$

So, the nullcline is a line. Sliding solutions exist for x values where the nullcline has k values between 0 and 1. When $k = 0$,

$$x_1 = \frac{\beta - \beta\varepsilon - \alpha}{\alpha\beta - \alpha}.$$

Alternatively, when $k = 1$,

$$x_2 = \frac{\beta - \beta\varepsilon - \alpha - \varepsilon}{\alpha\beta - \alpha}.$$

Therefore, we can conclude that there is never more than one sliding solution, and that this sliding solution is confined to the interval between x_1 and x_2, the order of which depends on the sign of ε.

The Filippov sliding region is calculated using the (x, y) system

$$\begin{aligned} \dot{x} &= 1 - x - kx \\ \dot{y} &= \beta - \beta\varepsilon - k\varepsilon - \alpha - (\beta + k)y - (\alpha\beta - \alpha)x \end{aligned}$$

where

$$k(y) = \begin{cases} 1 & y > 0 \\ 0 & y < 0. \end{cases}$$

The boundaries of the Filippov sliding region are places where the vector fields are tangent to the splitting manifold $y = 0$, i.e. where $\dot{y} = 0$, along $y = 0$. For the upper vector field, when $k = 1$, the tangency is given by the equation

$$\beta - \beta\varepsilon - \varepsilon - \alpha - (\alpha\beta - \alpha)x = 0.$$

It is immediately obvious that this is the same equation used to find the boundary of the nullcline above. Likewise, the tangency for the lower vector field, when $k = 0$, is given by the equation

$$\beta - \beta\varepsilon - \alpha - (\alpha\beta - \alpha)x = 0.$$

So, we see that the Filippov sliding region also exists only on the interval between x_1 and x_2, the order of which again depends on the sign of ε. We can conclude that no sliding solutions exist outside the Filippov sliding region. □

Chapter 8

Discussion

In this work we have completed a nonsmooth analysis of Welander's ocean convection model. In the case of the fused focus bifurcation, we can rigorously connect the nonsmooth bifurcation to its smooth counterpart. However, for the border collision bifurcation, there does not seem to exist a smooth bifurcation which is completely analogous. Instead, the border collision is the limiting bifurcation of two different smooth phenomena; a subcritical Hopf bifurcation and a periodic orbit saddle node. The homoclinic structure of the nonsmooth bifurcation seems to be a remnant of strong compression of the trajectories in the smooth system, as $a \to 0$. However, it is not clear that this smooth situation is the unique scenario which limits to the border collision bifurcation, and indeed there is some indication that it is not unique. So, this result raises several further mathematical questions. Perhaps the most immediate of these questions is whether a method similar to the blow up method of the fused focus can be found for the border collision. Then, instead of simply describing the analysis of a specific model, there might be some hope of generally describing systems which limit to a border collision bifurcation. For the fused focus, this work gives some indication of general conditions under which a supercritical Hopf bifurcation perturbs from the fused focus. A more general theory for this scenario would also be an interesting future direction.

There are several important nonsmooth dynamics questions which have also been brought into relief by this work. The scenario in which a border collision occurs with both persistence of the equilibrium and a change in stability is a new phenomenon, and has not been included in attempts to classify nonsmooth border collisions. This

indicates that classification of nonsmooth bifurcations is nowhere near complete, and also that those who have attempted to classify them have made hidden assumptions which may not be justified. In the case of the border collision, the assumption is that topological equivalence preserves the information necessary to the classification. This is seen by the transformation of one of the vector fields to be locally vertical, which destroys the stability change in Welander's model. So, this assumption is damaging to understanding the bifurcation in Welander's model. It's not clear what the essential mathematical structure will be, but examples like this show that care is absolutely essential in the approach to bifurcation classification.

The border collision bifurcation also raises some philosophical questions. In this case the bifurcation did not have a direct analogue to a smooth bifurcation, which makes one wonder what other types of strange behavior can be seen in nonsmooth systems, which have not been previously seen. It's possible that an attempt to find all such possibilities will be too vast an undertaking to be practical. In that case, do these nonstandard behaviors have any relevance, and is the relevance unique to each individual application, or can a more general mathematical theory be developed? Because a mathematically rigorous approach to nonsmooth dynamics is in its infancy, only time will make it clear which questions and approaches have any mathematical and practical value.

Aside from the mathematical implications of this analysis, there are some relevant climate implications. This work gives a mechanism for creating and destroying internally driven oscillations in the ocean system. If the parameters can be compared to physically relevant quantities, this could give an indication of impending transitions in the strength of the north Atlantic circulation. Because of the abrupt destruction of the oscillation due to the border collision bifurcation in the model, it is also possible that the transition between states could be both abrupt and catastrophic, without the warning signs that scientists normally look for in predicting these changes. Additionally, the oscillations seem to be critically dependent on the switching mechanism, with a more gradual transition between convective and nonconvective states destroying the oscillation. So, in this model at least, this gives some insight into the causes of oscillatory behavior in ocean convection which may be relevant to the real ocean system.

References

[1] Henk A Dijkstra. *Nonlinear physical oceanography: a dynamical systems approach to the large scale ocean circulation and El Nino*, volume 28. Springer Science & Business Media, 2005.

[2] Michel Crucifix. Oscillators and relaxation phenomena in pleistocene climate theory. *Phil. Trans. R. Soc. A*, 370(1962):1140–1165, 2012.

[3] K. Sakai and W.R. Peltier. A dynamical systems model of the dansgaard-oeschger oscillation and the origin of the bond cycle. *Journal of climate*, 12(8):2238–2255, 1999.

[4] Thierry Huck, Alain Colin de Verdière, and Andrew J Weaver. Interdecadal variability of the thermohaline circulation in box-ocean models forced by fixed surface fluxes. *Journal of physical oceanography*, 29(5):865–892, 1999.

[5] Ka-Kit Tung and Jiansong Zhou. Using data to attribute episodes of warming and cooling in instrumental records. *Proceedings of the National Academy of Sciences*, 110(6):2058–2063, 2013.

[6] Xianyao Chen and Ka-Kit Tung. Varying planetary heat sink led to global-warming slowdown and acceleration. *Science*, 345(6199):897–903, 2014.

[7] Hans Kaper and Hans Engler. *Mathematics and climate*. Siam, 2013.

[8] P. Welander. A simple heat-salt oscillator. *Dyn. Atmos. Oceans*, 6(4):233–242, 1982.

[9] P. Cessi. A simple box model of stochastically forced thermohaline flow. *Journal of physical oceanography*, 24(9):1911–1920, 1994.

[10] F. Dercole, A. Gragnani, and S. Rinaldi. Bifurcation analysis of piecewise smooth ecological models. *Theor. Popul. Biol.*, 72(2):197–213, 2007.

[11] I Eisenman and JS Wettlaufer. Nonlinear threshold behavior during the loss of arctic sea ice. *Proceedings of the National Academy of Sciences*, 106(1):28–32, 2009.

[12] H. Stommel. Thermohaline convection with two stable regimes of flow. *Tellus*, 13:224, 1961.

[13] A. F. Filippov and F. M. Arscott. *Differential Equations with Discontinuous Right-hand Sides: Control Systems*, volume 18. Springer, 1988.

[14] Y. A. Kuznetsov, S. Rinaldi, and A. Gragnani. One-parameter bifurcations in planar filippov systems. *Int. J. Bifurcat. Chaos*, 13(08):2157–2188, 2003.

[15] M. di Bernardo, C. Budd, A. R. Champneys, and P. Kowalczyk. *Piecewise-smooth dynamical systems: theory and applications*, volume 163. Springer, 2008.

[16] M. R. Jeffrey. Nondeterminism in the limit of nonsmooth dynamics. *Phys. Rev. Lett.*, 106(25):254103, 2011.

[17] M. R. Jeffrey. Hidden dynamics in models of discontinuity and switching. *Physica D*, 273:34–45, 2014.

[18] A. Colombo, M. Di Bernardo, S. J. Hogan, and M. R. Jeffrey. Bifurcations of piecewise smooth flows: Perspectives, methodologies and open problems. *Physica D*, 241(22):1845–1860, 2012.

[19] M. Guardia, T. M. Seara, and M. A. Teixeira. Generic bifurcations of low codimension of planar filippov systems. *J. Differ. Equations*, 250(4):1967–2023, 2011.

[20] O. Makarenkov and J. S. W. Lamb. Dynamics and bifurcations of nonsmooth systems: A survey. *Physica D*, 241(22):1826–1844, 2012.

[21] K Uldall Kristiansen and SJ Hogan. Regularizations of two-fold bifurcations in planar piecewise smooth systems using blowup. *SIAM Journal on Applied Dynamical Systems*, 14(4):1731–1786, 2015.

[22] J Sotomayor and MA Teixeira. Regularization of discontinuous vector fields. In *International Conference on Differential Equations, Lisboa*, pages 207–223, 1996.

[23] M. A. Teixeira and P. R. da Silva. Regularization and singular perturbation techniques for non-smooth systems. *Physica D*, 241(22):1948–1955, 2012.

[24] Claudio A Buzzi, Paulo R da Silva, and Marco A Teixeira. A singular approach to discontinuous vector fields on the plane. *Journal of Differential Equations*, 231(2):633–655, 2006.

[25] Jaume Llibre, Paulo R da Silva, and Marco A Teixeira. Study of singularities in nonsmooth dynamical systems via singular perturbation. *SIAM Journal on Applied Dynamical Systems*, 8(1):508–526, 2009.

[26] Richard McGehee. Triple collision in the collinear three-body problem. *Inventiones mathematicae*, 27(3):191–227, 1974.

[27] C. Jones. Geometric singular perturbation theory. *Dynamical systems*, pages 44–118, 1995.